5-2009

Comparison of Data Collection and Methods For the Approximation of Streambed Thermal Properties

Jonathan D. Bingham
Utah State University

COMPARISON OF DATA COLLECTION AND METHODS FOR THE APPROXIMATION OF STREAMBED THERMAL PROPERTIES

by

Jonathan D. Bingham

A thesis submitted in partial fulfillment
of the requirements for the degree

of

MASTER OF SCIENCE

in

Civil and Environmental Engineering

Approved:

Dr. Bethany T. Neilson Major Professor	Dr. David K. Stevens Committee Member
Dr. Gilberto E. Urroz Committee Member	Dean Byron R. Burnham Dean of Graduate Studies

UTAH STATE UNIVERSITY

Logan, Utah

2009

ABSTRACT

Comparison of Data Collection and Parameter Estimation Techniques for the Approximation of Streambed Thermal Properties

by

Jonathan D. Bingham, Master of Science

Utah State University, 2009

Major Professor: Dr. Bethany T. Neilson
Department: Civil and Environmental Engineering

When approximating heat transfer through a streambed, an understanding of the thermal properties of the sediments is essential (e.g., thermal conductivity, specific heat capacity, and density). Even though considerable research has been completed in this field, little has been done to establish appropriate standard data collection approaches or to compare modeling methods for approximating these properties. Three mixture models were selected for comparison against each other and against a bed conduction model (SEDMOD). Typical data collection approaches were implemented for use in the mixture models while numerous data collection approaches were employed for use within SEDMOD. Sediment samples were taken from the streambed to estimate the necessary parameters for the mixture models (e.g., sediment volume, density, porosity, etc.) and to identify the minerals present. To yield more accurate estimates of the thermal properties from SEDMOD, methods of obtaining sediment temperature profiles representing the

influences of conduction only were developed through the use of a steel cylinder and different capping materials (e.g., using geo-fabric or aluminum).

In comparison to laboratory measurements of the thermal properties, it was found that the mixture model that provided the best estimates of the thermal properties was a volume weighted average. The method that best isolated conductive heating from advective heating was the steel cylinder with an aluminum cap. Using this data to calibrate SEDMOD yielded thermal diffusivity values most similar to the laboratory measurements. Due to its ability to estimate both thermal diffusivity and reproduce sediment temperature profiles, SEDMOD is recommended in combination with the aluminum isolation technique.

(108 pages)

To my dear wife Stacey, whose love and support have carried us to this goal,

I also wish to dedicate this work to our son Ammon.

ACKNOWLEDGMENTS

A great man once said, “We are the product of lives who have touched ours.” In my life I have found this to be true. I would like to take a few lines and recognize the lives that have touched mine in helping me finish this work.

I would like to thank my advisor, Bethany Neilson, who amid her demanding schedule found time to take a chance on this student and teach me along the way. I would also like to thank my other committee members, Drs. Stevens and Urroz. They have helped teach me the needed lessons to write this thesis.

Work such as this requires much effort in writing and analyzing the data but just as much exertion goes into collecting the necessary field data. My field crews have included Dr. Bethany Neilson, Noah Schmadel, Quinten Bingham, Andrew Hobson, Oscar Marquina, and Camilla Lyman. Many hands make light work, or in the case of heavy work such as this they make it possible.

This research would not have even been possible without the beautiful stream studied. The Utah Division of Wildlife Resources is to be thanked for their willingness to allow us to collect data on Curtis Creek. Hardware Ranch Manager Dan Christensen and his team were very helpful in providing information and even in providing a helping hand when needed. Dr. John Carter was invaluable in teaching us practical sediment sampling techniques used in literature as well as loaning us some of his sampling equipment for a time.

Most importantly I would like to thank those who have brought me to this point and supported me through it, my family. I thank my dear mother and father whose loving support and firm admonition have brought me to a college education. To grandparents

and extended family who have encouraged me along the way. Finally and most importantly I would thank my dear companion Stacey, whose prayers, encouragement, and goodness have made all the difference.

Finally I would thank God for so many prayers answered and blessings given, for the strength to overcome and patience to endure.

Jonathan D. Bingham

CONTENTS

Page

LIST OF TABLES

LIST OF FIGURES

CHAPTER 1

INTRODUCTION

Water temperature in river systems is an important characteristic of aquatic communities. Even seemingly slight changes in average stream temperature or seasonal and diel fluctuations can directly affect the life cycles, metabolic rates, growth and mortality of organisms living within the system [*Allen*, 1995]. Water temperature can also affect the productivity and nutrient cycling within an aquatic ecosystem [*Allen*, 1995; *Poole and Berman*, 2001]. The temperature of streams has been shown to be the result of many hydrological and ecological processes [*Poole and Berman*, 2001; *Webb and Zang*, 1997]. Stream temperature models have been constructed which have established relationships for quantifying stream-atmosphere fluxes through the use of weather data [*Chapra et al.*, 2004; *Evans et al.*, 1998; *Healy and Ronan*, 2003; *Morse*, 1970; *Neilson*, 2006; *Sinokrot and Stefan*, 1993, 1994]. Nevertheless, the discussion continues as how to best quantify the stream-sediment component of the heat budget. *Constantz* [2008] states that four major mechanisms are responsible for the streambed portion of the heat balance. These include radiation, conduction, convection, and advection. Constantz goes on to state that one or two of these mechanisms generally dominate the temperature patterns of the streambed. Many researchers (e.g., *Silliman and Booth* [1993]) consider the dominant streambed fluxes to be that of advection and conduction within the streambed. Of these two mechanisms, conduction has received much of the attention in modeling [*Boyd and Kasper*, 2003; *Chapra et al.*, 2004; *Morse*, 1970; *Sinokrot and Stefan*, 1993]. To quantify bed conduction, these models have used Fourier's Law (Equation 1-1) or the Conduction Equation (Equation 1-2).

$$\frac{q_z}{A} = -k\frac{dT}{dz} \tag{1-1}$$

q_z = heat flow in the z direction (W), A = cross sectional area perpendicular to the z direction (cm^2), k = thermal conductivity (W/(cm ºC)), z = direction and depth of the heat transfer (cm), T = temperature of the media at depth (ºC).

$$\frac{\partial T}{\partial t} = \alpha\frac{\partial^2 T}{\partial z^2} \tag{1-2}$$

t = time (seconds), z = depth (cm), α = thermal diffusivity of the sediment (cm^2/s). Thermal diffusivity is related to thermal conductivity as shown in Equation 1-3.

$$\alpha = \frac{k_{total}}{\rho_b \cdot C_p} = \frac{k_{total}}{C_v} \tag{1-3}$$

C_p = specific heat capacity (J/(g °C)), C_v = volumetric heat capacity ($J/(cm^3$ °C)), ρ_b = bulk density of the material (g/cm^3).

Equations 1-1 to1-3 show that in order to quantify streambed conduction, variables such as bulk density, thermal conductivity, specific heat capacity, or thermal diffusivity must be known.

The manner by which these equations are populated varies widely. Literature values are often used as a source for these thermal properties. Table 1-1 shows a compilation of thermal properties for sediment materials from a variety of literature sources and highlights some of the difficulties associated with using literature values.

First, many literature sources give only a common name of the material which leaves the modeler to use their judgment in selecting the material that matches the streambed of interest. Furthermore, there are duplicate minerals from different literature sources that provide different values. These differences in property values are possibly due to geologic differences in source material, measurement methods, saturation, density, etc. A final difficulty with using literature values is the heterogeneity in size and makeup of streambed sediments. All of these complicate the task of selecting thermal properties for the calculation of streambed conduction.

Table 1-1. Common Thermal Properties Found in Literature. Shown Are the Common Name of the Material, Thermal Conductivity, Thermal Diffusivity, Bulk Density, Specific Heat and the Reference from Which It Came

Material	Conductivity k (W/m ºC)	Thermal Diffusivity α (cm^2/s)	Density ρ (g/cm^3)	Specific Heat C_p (J/g ºC)	Reference
Mud Flat	1.82	4.80E-03	-	-	8
Sand	2.5	7.90E-03	-	-	8
Sand	-	-	1.52	0.8	1
Mud Sand	1.8	5.10E-03	-	-	8
Mud	1.7	4.50E-03	-	-	8
Sandstone	2.9	-	2.15	0.745	2
Wet Sand	1.67	7.00E-03	-	-	9
Rock	1.76	1.18E-02	-	-	11
Rock	0.606-4.02	-			4
Stone	-	-	1.5	0.8	1
Loam (75% Sat)	1.78	6.00E-03	-	-	10
Wet Soil	1.8	4.50E-03	1.81	2.20	7
Gelatinous Sediments	0.46	2.00E-03	-	-	12
Concrete Canal	1.55	8.00E-03	2.2	0.88	12
Granite	2.89	1.27E-02	2.7	0.85	7
Granite	2.79	-	2.63	0.775	2
Limestone	-	-	1.65	0.909	1
Limestone	2.15	-	2.32	0.81	2
Limestone	1.43	-			5
Calcite	3.59	-			4
Calcite		-	2.71		6
Quartzite	5.38	-	2.64	1.105	2
Quartz	8.8	-	-	-	3
Quartz		-	2.65		6
Quartz	7.69	-	2.647		4
Clay	-	-	1	0.92	2
Dolomite	5.51	-	2.857		4
Dolomite		-	2.87		6
Kaolonite	2	-	2.63		6
Water	0.59	1.40E-03	1	0.999	7
Water	0.6	-			6

1) [*Cengel and Boles*, 2002]
2) [*Incropera et al.*, 2007]
3) [*Or et al.*, 2008]
4) [*Horai*, 1971]
5) [*Touloukian and Buyco*, 1970]
6) [*Brigaud and Vasseur*, 1989]
7) [*Cengel*, 1998], [*Bejan*, 1993; *Grigull and Sandner*, 1984; *Mills*, 1992]
8) [*Andrews and Rodvey*, 1980]
9) [*Geiger*, 1965]
10) [*Nakshabandi and Kohnke*, 1965]
11) [*Carslaw and Jaeger*, 1959; *Chow et al.*, 1988]
12) [*Hutchinson*, 1957]

In order to deal with the heterogeneous nature of sediments, mixture models have been developed that use a sediment property (such as constituent volume or bulk density) as a basis of a relationship to calculate an overall thermal property (e.g., thermal conductivity or volumetric heat capacity). Most mixture models use literature values of the different sediment components in order to calculate total thermal conductivity or volumetric heat capacity [*Boyd and Kasper*, 2003; *Or et al.*, 2008; *Zang et al.*, 2007], while other models are based on characteristics such as porosity or bulk density and are purely empirical [*Campbell*, 1985].

In an effort to account for the heterogeneity and different properties of the sediment mix, some research has sought to calculate these thermal parameters through calibration of sediment conduction models. This parameter estimation approach uses sediment temperature data collected at different depths as calibration data. The success of this approach is dependent on consistencies between the model assumptions and the data collection. For example, these bed conduction models are generally built using a numerical approximation of Fourier's Law (Conduction Equation) (Equations 1-2). As has been stated, this equation accounts only for heat transfer due to conduction. It is very important that the temperature data used in these applications match the assumptions made in the model equations. Past efforts have shown that just installing temperature instrumentation in the streambed or even isolating instrumentation from either vertical or horizontal advective flows does not yield temperature data representing conductive heating only [*Neilson*, 2006; *Silliman and Booth*, 1993]. The work by *Neilson* [2006] showed that data collected which did not completely isolate conduction could yield

thermal diffusivity values nearly an order of magnitude lower than those shown in literature.

These different modeling and literature methods have been established in search of the most accurate estimation of bed conduction parameters due to their significance in instream temperature predictions. More recently, these parameters have been used with observed sediment temperatures to quantify seepage from the stream [*Constantz*, 1998, 2008; *Constantz et al.*, 2002; *Hatch et al.*, 2006; *Ronan et al.*, 1998]. More accurate estimates of the sediment thermal properties will likely result in more accurate estimations of instream temperature predictions and seepage losses.

Due to the importance of streambed conduction parameters in research, and the apparent lack of comparisons between the methods commonly used to estimate them, this research seeks to:

1. Use established installation techniques to install temperature probe arrays to monitor uninfluenced sediment temperature profiles as well as build on the research of *Neilson et al.* [2009] and *Silliman and Booth* [1993] to physically block advective flows to monitor only conductive heating of the streambed. These isolated temperature time-series will then be used as calibration data for a bed conduction model to estimate thermal diffusivity of sediments.
2. Sample streambed sediments to determine properties such as particle distribution, bulk density, and volumetric water content. Use this sediment data in conjunction with literature thermal properties to

populate mixture models to calculate thermal conductivity and diffusivity for comparison with estimates from Objective 1.

3. Compare laboratory results of sediment thermal properties with those of the conduction model and mixture models. Make recommendations of most accurate estimation methods by their ability to match laboratory measurements.

CHAPTER 2

DATA COLLECTION METHODS FOR USE IN THE ESTIMATION OF STREAMBED THERMAL PROPERTIES

Abstract

Past instream temperature modeling research has been successful in forming relationships that define water-atmospheric energy fluxes, however, streambed fluxes typically are not as thoroughly considered or validated. In the past, simple heat transfer equations have been used to approximate bed conduction. When modeling bed conduction, the necessary thermal properties are often taken from literature; while others have used sediment temperature profiles to calibrate bed conduction models to approximate these properties. This research explores different methods of installing temperature probes into cobble bed sediments that do not create preferential flow paths. These methods are then used to develop an approach to collect sediment temperature data that represent heating due to only conduction. Installation methods included digging a hole in the streambed and the use of a spike and sleeve. It was found that the spike and sleeve installation method induced the least preferential flow into the sediments. Steel cylinders with two different capping materials (aluminum cap and geo-fabric) were used to isolate conductive heating in the bed sediments. The aluminum effectively blocked all flow through the sediments, but showed possible problems with solar heating and a small stagnant layer of water between the cap and the sediments. The geo-fabric allowed some flow through the cylinder which eliminated the stagnant water layer, but may limit the

ability to estimate thermal properties accurately under certain conditions, due to an increase in seepage over time.

Introduction

Of the stream sediment interactions, the role of bed conduction on the stream energy balance has been debated. Historically, bed conduction in stream temperature models was considered negligible due to prior studies of heat exchange in lakes [*Jobson*, 1977]. These studies showed that the contribution of energy from bed conduction was insignificant in larger bodies of water such as deep lakes. It has since been found that bed conduction can be an important component of heat transfer in shallow lakes and even more so in small streams [*Hondzo et al.*, 1991; *Tsay et al.*, 1992; *Webb and Zang*, 1997]. For example, in the smaller, shallower Clearwater River, *Sinokrot and Stefan* [1993] found conduction to be just as important as the other thermal fluxes for certain time periods.

To quantify the effects of bed conduction, some researchers have built or used models focused on streambed processes [*Healy and Ronan*, 2003; *Hondzo and Stefan*, 1994; *Jobson*, 1977], while others have adopted a more inclusive stream energy balance approach [*Boyd and Kasper*, 2003; *Chapra et al.*, 2004; *Neilson*, 2006; *Sinokrot and Stefan*, 1993]. All of the models mentioned use heat transfer equations such as Fourier's Law or the Conduction Equation to estimate heat conduction through a homogeneous slab. Some of the data and parameters required to solve these equations are: water column temperature that is either measured or predicted, sediment bulk density, specific heat, thermal diffusivity of the sediment layer, and if possible for calibration purposes, temperature at various depths in the sediment. Water column and bed substrate

temperatures can be measured in-situ in a straight forward manner, but details such as specific heat, bulk density, thermal conductivity, and thermal diffusivity of the saturated sediment are more difficult to determine.

One of the common methods used to find appropriate values for bulk density, specific heat, and thermal diffusivity is through the use of literature values based on the observed sediment type [*Chapra et al.*, 2004; *Morse*, 1970; *Sinokrot and Stefan*, 1994; *Stonestrom and Blasch*, 2003]. Another approach is to select literature values as an initial estimate and adjust these parameters until a bed conduction model output mimics the observed sediment temperature data [*Constantz*, 1998; *Constantz et al.*, 2002; *Neilson*, 2006; *Sinokrot and Stefan*, 1993].

In this latter approach, there are potential errors associated with adjusting parameters such as thermal diffusivities to yield representative predicted bed sediment temperature. Often the data collection method implemented and the associated model assumptions do not coincide. For example, to calculate thermal diffusivity of the sediments of the Virgin River, *Neilson* [2006] used the heat conduction model SEDMOD (Dr. Steven Chapra, Medford, MA) which is a numerical approximation of the Heat Conduction Equation (Equation 2-1).

$$\frac{\partial T}{\partial t} = \alpha \frac{\partial^2 T}{\partial x^2} \tag{2-1}$$

T = temperature (°C), t = time (seconds), x = depth (cm), α = thermal diffusivity of sediments (cm^2/s). This equation approximates heat transfer due to only conduction and provides a method for estimating thermal diffusivity based on observed sediment

temperature profiles. *Neilson* [2006] and *Neilson et al.* [2009] point out that the temperature data collected in sediments often include the influences of advective flows in addition to conduction at some locations. This suggests that in order to estimate bed conduction parameters, the influences of advective fluxes must be excluded from the bed sediment temperature measurements. However, once the thermal properties of the sediments are established, the sediment temperature data that represent the confounded effects of conduction and advection can be used to estimate seepage rates [*Constantz et al.*, 2002; *Constantz*, 2008; *Hatch et al.*, 2006; *Stonestrom and Blasch*, 2003].

Neilson et al. [2009] initially attempted to separate out the effects of the two fluxes by placing one temperature probe array in the sediment to measure all fluxes while a steel cylinder was placed around the sediment containing another temperature probe array to monitor conduction. They found, however, that vertical advective fluxes can take place within these cylinders, influencing their ability to estimate thermal diffusivity of the bed.

To determine the most accurate methods of collecting temperature data for use with bed conduction models, this paper identifies a method of installing temperature probes that precludes preferential flow (advective flow). This installation method is used with different conduction isolation techniques in an attempt to monitor bed sediment temperature variations due only to conduction. In conjunction with the sediment temperature data collected, sediment sampling and vertical hydraulic gradient data were also collected to assist in explaining some of the potential processes influencing sediment temperatures. The resulting temperature time-series and sediment samples will be used in the parameter estimation methods discussed in Chapter 3.

Site Description

The stream selected for this research was Curtis Creek in Northern Utah, on the Hardware Ranch Wildlife Management Area. The location of the ranch is about 24 kilometers east of the City of Hyrum in Cache County, Utah (Figure 2-1). The property is owned by the State of Utah and is used as wildlife habitat and a winter feeding ground for the local Rocky Mountain Elk population. Prior to the state acquiring the land, the property had several owners, mostly made up of homesteaders or ranchers. Anthropogenic use of stream water is currently limited to stock watering and flood irrigation. In recent history, the State of Utah used federal grant money for a stream relocation project that moved a section of the creek away from their animal corrals [D. *Christensen*, personal communication June 22, 2007]. The river reach considered in this study is about 1.5 km in length, stretching roughly from Laketown Road to state Highway 101 (Figure 2-1).

Curtis Creek is a high gradient mountain stream with an average bed slope of 2% and an average bankfull width of 3.7 m. The bed material of the stream consists of mostly gravel and cobble sized rock (2 -15 cm diameter). The study reach is highly influenced by groundwater, consisting of both groundwater/surface water interactions as well as overland flow from surface seeps to the creek.

Ten data collection locations (referred to as "cross sections") were selected where instream temperatures were monitored, and sediment samples and vertical hydraulic gradient data were collected. Figure 2-1 shows the distribution of these cross sections. The data collection sites are designated by their position downstream from the uppermost

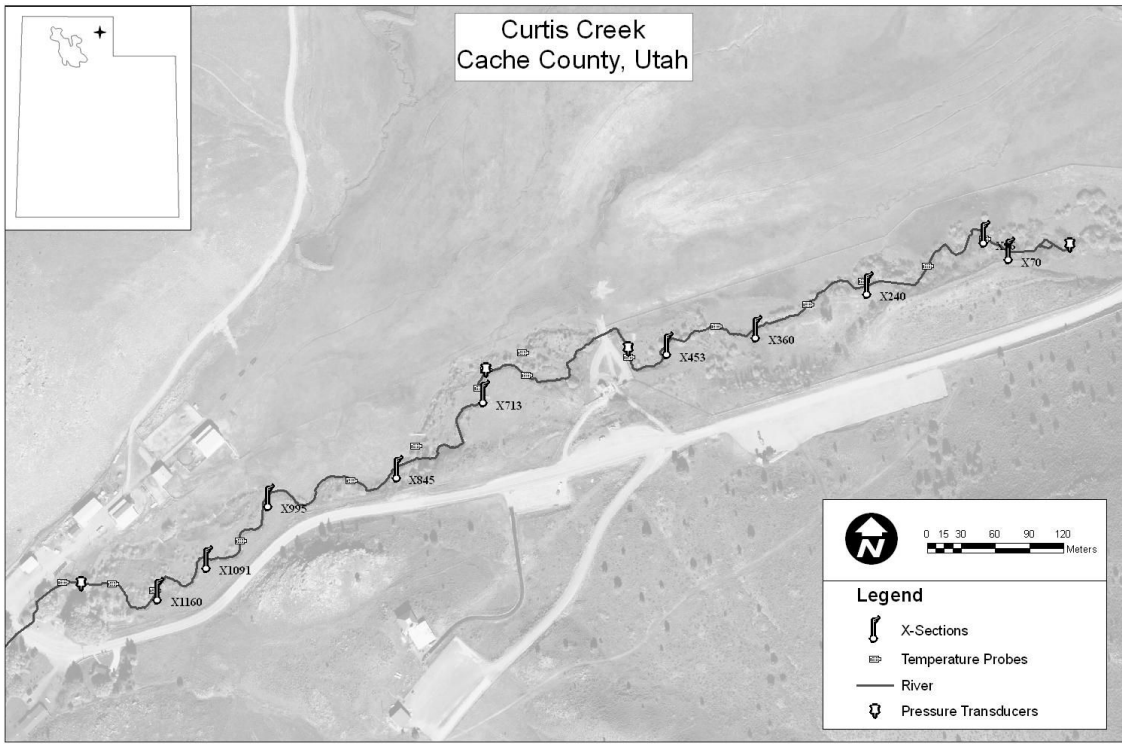

Figure 2-1. Study reach at Curtis Creek, Utah, showing data sampling locations.

flow gauge (i.e., X1160 is the cross section found 1160 meters downstream of the uppermost gauging station of the study reach).

Data Collection Methods

Constantz [2008] states that there are four heat fluxes within a streambed, namely those of conduction, advection, convection, and radiation; however, generally one or two of the fluxes will dominate. The data collection methods in this research considered conduction and advection as the governing heat fluxes in the sediments of Curtis Creek.

Temperature Probe Array Installation

Guided by the methodology of *Neilson et al.* [2009], sediment temperature profiles were collected by attaching three HOBO® Temp Pro V2 temperature probes

(Onset Computer Corporation, Bourne, MA) to pieces of rebar so as to position them at 3, 9 and 20 cm below the stream-sediment interface (referred to as a "temperature probe array" throughout). After these temperature probe arrays were placed in the streambed, a fourth temperature probe was secured to the rebar protruding from the streambed at approximately 0.6 of the water depth. This enabled the monitoring of the main channel temperature (which is assumed to be the boundary temperature at the sediment surface).

The initial installation technique was applied from July 17, 2007 to August 1, 2007. During this period the sediment temperature probe arrays were installed by digging a hole in the streambed to a depth of 20 cm, stockpiling the sediment, then placing the array in the hole and burying it using the stockpiled material (referred to as "Installation Method 1" throughout).

The data resulting from Installation Method 1 suggested that the method actually induced preferential flow through the sediment. Based on these results, a new installation method was applied. Installation Method 2 was a variant of the spike and sleeve technique found in other research applications [*Baxter and Hauer*, 2003; *Constantz et al.*, 2002; *Stonestrom and Blasch*, 2003]. A spike, roughly 7.5 cm in diameter, and a hollow steel sleeve just large enough to slide over the spike were fabricated to accommodate a piece of rebar with the three Hobo® temperature probes attached. The spike was driven to a depth of 20 cm in the streambed. The hollow sleeve was then slid over the spike and driven into the streambed sediment to the same depth. With the sleeve in place, the spike was removed leaving a 7.5 cm diameter hole where the temperature probe array could be inserted. Once it was verified that the probes were at the proper depth, the sleeve was removed, allowing the sediments to settle back around the temperature probes, leaving

the streambed in relatively "pre-installation" condition. This installation method was used from August 2007 to October 2007 and again in June 2008 through August 2008. Table 2-1 shows the locations where temperature probe arrays were placed using Installation Methods 1 and 2. These temperature probe arrays are assumed to measure sediment heating due to advection and conduction.

Bed Conduction Isolation

To ensure that the heating of bed sediments was primarily due to conduction, some consideration was taken to impede advective heating caused by hyporheic flow and groundwater-surface water exchange through the sediment. As has been mentioned, *Neilson et al.* [2009] developed methods to separate heat exchange due to conduction from that of advection by placing one temperature probes array in the sediment without any protection (Figure 2-2(a)) and another temperature probe array was installed within a steel cylinder (Figure 2-2(b)).

Table 2-1. Data Collection Locations

Method/Location	X70	X96	X240	X360#	X453	X713	X845	X995#*	X1091	X1160
Temperature Array	X	X	X	X	X	X	X	X	X	X
Conduction Isolation		X	X			X		X		X
Sediment Sampling		X	X			X		X		X
Piezometers		X	X	X		X		X		X

** At this location two steel cylinders were installed for the comparison of isolation techniques*
 # These locations were newly installed for the 2008 data collection season

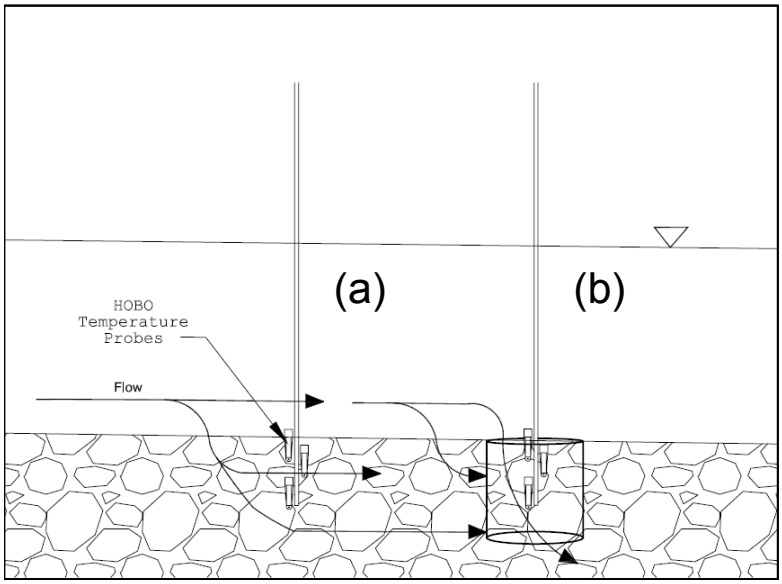

Figure 2-2. Temperature probe array installation.

It was hypothesized that the probes within the cylinder (Figure 2-2(b)) would measure the thermal flux caused only by conduction while the other probes (Figure 2-2(a)) would measure the confounded effects of conduction and advection. Vertical flow through the cylinder was found to be the main limitation to this design. To address this issue in the current research, a series of caps were designed to hinder vertical water flow through the cylinder. One of the concerns of using these capping techniques was the need to minimize the thermal resistance that the capping material and the water layer between the cap and the sediment might add. To quantify the potential resistance, a worse case scenario was analyzed where larger substrate prevented the complete insertion of the cylinder, leaving a lip protruding into the stream about 4 cm. Calculations using Equation 2-3 show that this water (thermal diffusivity = 1.4×10^{-7} m^2/s) filled headspace could cause a heat transfer lag of 190 minutes. With data being collected at ten minute intervals, this thermal resistance would create a lag in the data collected in the sediments beneath this layer, emphasizing the need to install the cylinder flush with the sediments.

$$t = \frac{L^2}{\alpha} \tag{2-3}$$

L = distance of heat transfer (m), α = thermal diffusivity of material (m^2/s), t = time for heat to transfer across boundary (seconds). With the possible thermal lag due to headspace, the properties of the capping material would also need to be considered and therefore, have to be carefully selected. The first cap material selected was Boom Environmental™ (Newtonville, MA) style 884 woven geo-textile fabric. This fabric was chosen for its low permeability as well as its white color. It was hypothesized that the permeable fabric would allow very limited exchange with the water column and prevent a stagnant area between the fabric and the sediment. This slow exchange was initially assumed to diminish the thermal lag from the inevitable headspace, albeit small in most installations, between the cap and the sediments. The thermal resistance of the fabric was also considered negligible as the permeation of water would set the top conduction boundary at the sediment surface and not the fabric surface. Therefore, the stream temperature could be used as a boundary condition in conduction modeling. It was assumed that the velocity vectors that could penetrate the fabric would not have a significant effect on the temperatures in the sediments and would primarily represent the heat transfer due to conduction (Figure 2-3(b)). White fabric was selected to avoid heating of the cap due to solar radiation penetrating the water column. The fabric was glued to a 5 cm diameter PVC pipe that slid over the rebar and the exposed top of the 3 cm temperature probe (Figure 2-3(c)).

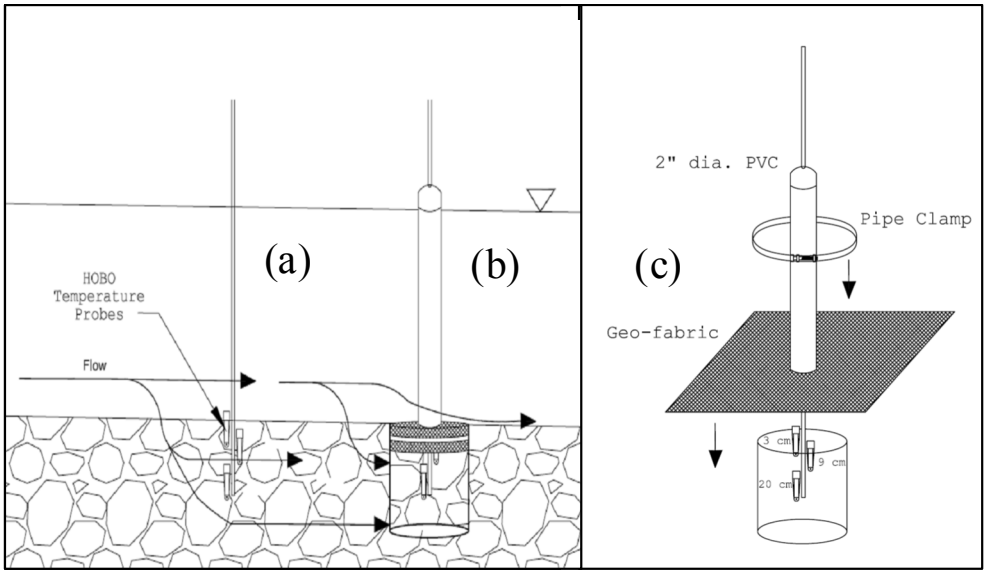

Figure 2-3. Steel cylinder installation with geo-fabric.

This precaution is to provide a water tight seal so no "plunging" of the water around the rebar or temperature probe array was possible. The remainder of the fabric was stretched over the cylinder and secured using a large pipe clamp (Figure 2-3(b) and (c)). These covered cylinders with their associated temperature probe arrays were deployed from June 2008 through August 2008. The isolation experiments were conducted at cross sections X96, X240, X713, X995, and X1160 (Table 2-1).

To test the hypothesis that the fabric minimized advective heat transfer to the sediments, an impervious aluminum cap was additionally tested as a standard for impeding flow. For this application, a thin aluminum cap was used. A hole was drilled in the top of the cap and a piece of PVC pipe was attached following the procedure used with the fabric cap. Any seams or joints in the aluminum were caulked with silicon to prevent seepage. The aluminum cap attached to the PVC was slid over the rebar and steel cylinder and secured using a large pipe clamp. Aluminum was selected for its high thermal diffusivity (97.1×10^{-6} m^2/s). Because aluminum has a much higher thermal

diffusivity than that of both water ($1.4x10^{-7}$ m^2/s) and sediment ($1.18x10^{-6}$ m^2/s), its affect could be neglected [*Chapra et al.*, 2004; *Incropera et al.*, 2007]. This assumption was further tested by calculating the transfer time for the cap using Equation 2-3, which was $3.41x10^{-4}$ seconds. As the temperature probes logged every ten minutes the transfer resistance time of the aluminum was insignificant. As a headspace as small as 1 cm of stagnant water between the cap and the sediment could cause a lag of almost 12 minutes, extra care was taken to minimize the space between the cap and sediment. This isolation technique was deployed from October 30, 2008 to November 11, 2008 at cross section X995. A cylinder capped with geo-fabric was also installed at this location for comparison of the two isolation methods.

Sediment Sampling

To acquire sediment samples, a thirty centimeter diameter stainless steel cylinder was fabricated (Figure 2-4). This sampling cylinder was pushed into the streambed to a depth of 22.5 cm. The resulting sediment core was taken from the interior of the cylinder in three equal layers of 7.5 cm.

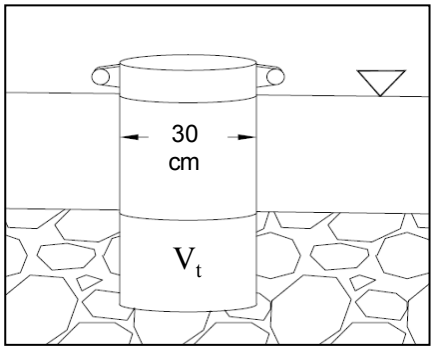

Figure 2-4. Sediment sampling technique. V_t is the total sample volume.

Sediment samples were separated according to particle size using soil sieves, according to ASTM standard D 422 – 63 [*ASTM*, 2007]. The sizes of sieves used were 6.35 cm, 2.54 cm, 1.27 cm, 0.64 cm, 0.47 cm, 0.24 cm, 0.08 cm, 0.02 cm, and 0.005 cm. After sieving, the sediment fractions were weighed using a Mettler Toledo® PL6001-S scale (Columbus, OH). Following weighing, fraction volumes were measured by submerging each of the size fractions separately in water and noting the change in volume of the mixture. Both mass and volume measurements will be used in Chapter 3, but for the purposes of this chapter, the mass and particle size data will be used to provide particle size distributions of the sediment. This data can be found in Appendix B.

While it is understood that advective heat fluxes influence sediment temperatures, the origin and destination of the flow will result in drastically different effects. For example, if stream water is flowing from the channel, through the sediment, and into groundwater, the temperatures at depth would mimic the instream temperatures. If the groundwater is upwelling into the channel, the sediment temperatures may more closely mimic those of groundwater. To gain a better understanding of where upwelling and downwelling in the streambed may be occurring, piezometers were installed at cross sections X96, X240, X360, X713, X995, and X1160 (Table 2-1). The piezometers were installed and the vertical hydraulic gradients calculated [*Baxter and Hauer*, 2003]. Figure 2-5 shows a diagram of the piezometer installation.

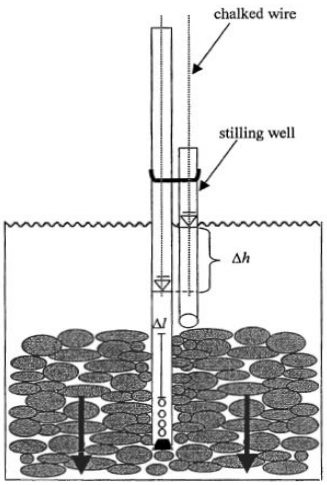

Figure 2-5. Piezometer installation diagram. This example shows downwelling, or water leaving the stream and entering groundwater. Adapted from [*Baxter and Hauer*, 2003].

Vertical hydraulic gradients were calculated using Equation 2-4.

$$VHG = \frac{\Delta h}{\Delta l} \tag{2-4}$$

VHG = vertical hydraulic gradient (dimensionless), Δh = difference in head between stream surface and water level in the piezometer (cm), Δl = distance from sediment surface to first opening in piezometer sidewall (cm). A positive vertical hydraulic gradient denotes a loss of water from the stream or downwelling, while a positive vertical hydraulic gradient denotes a gain to the stream or upwelling

Results

Temperature Probe Array Installation

After temperature, sediment, and vertical hydraulic gradient information were collected, time periods which exhibited stable temperature patterns were selected to compare the installation and isolation methods. Figure 2-6 shows the temperature results from Installation Method 1 from 7/28/08 to 7/31/08. Main channel temperatures are plotted along with temperatures at depths of 3, 9, and 20 cm within the sediment. Notice that Figure 2-6 (a) and (b) show similarities between the temperatures at the 3 and 9 cm depths for a three day period, while Figure 2-6 (c) and (d) show a decrease in temperature amplitude with depth. Consistent amplitude with increase in depth could be an indication of downwelling due to hyporheic or groundwater exchange or preferential flow caused by the installation method.

Figure 2-7 shows the temperature time-series resulting from Installation Method 2 at the same locations shown in Figure 2-6 with the addition of cross section X995. These plots show three days of temperature data for the main channel, 3, 9, and 20 cm sediment depths during 7/28/08 to 7/31/08. Considerable differences can be seen in temperature distributions within the sediment throughout the study reach. All of the cross sections show a decrease temperature amplitude and larger time lag with an increase in depth, however, the extent of these vary by cross section. These differences may be due to the variability of the sediment from location to location, or differing amounts of groundwater intrusion or hyporheic exchange.

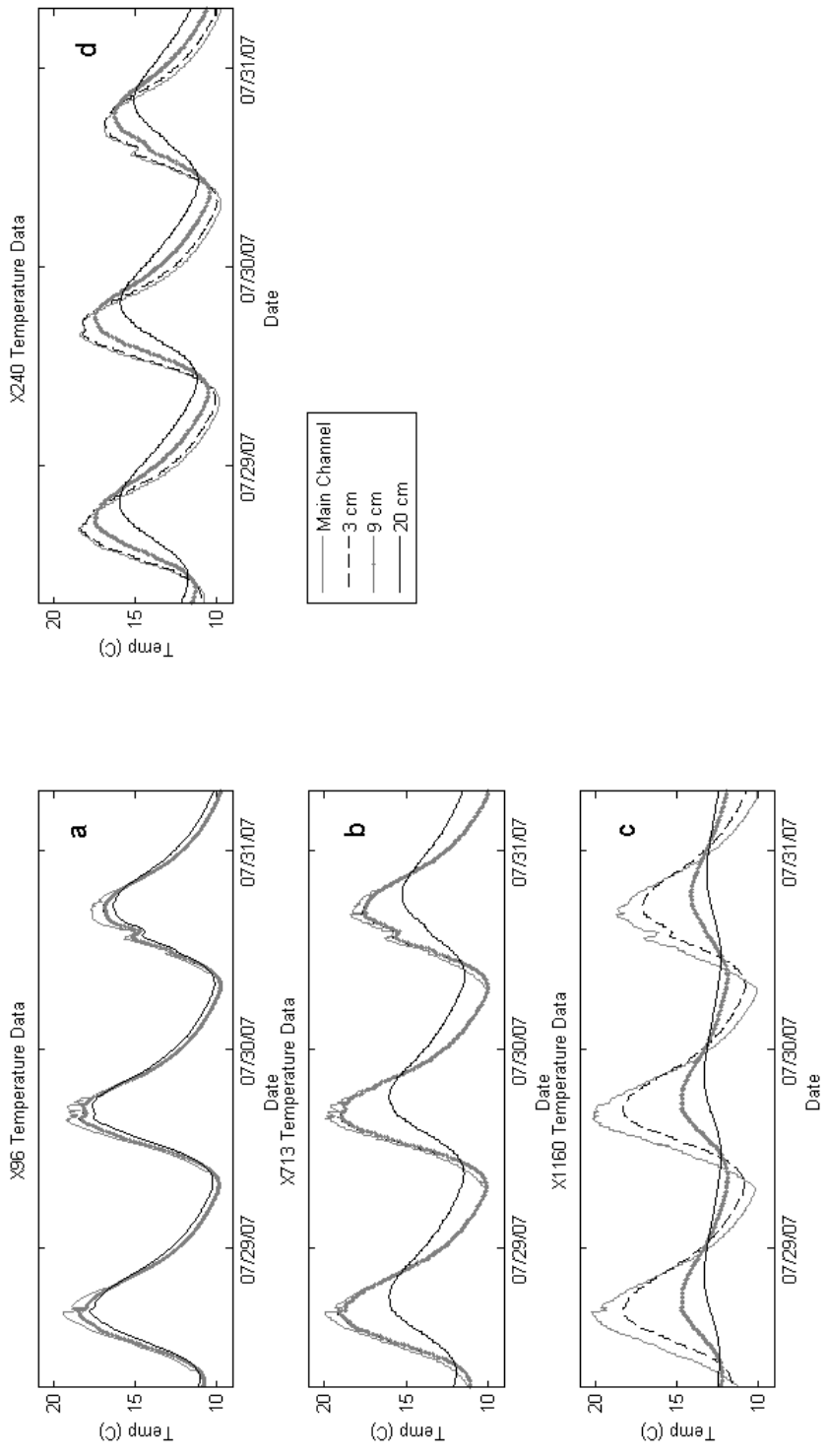

Figure 2-6. Temperature time-series results from Installation Method 1 for cross sections X96 (a), X713 (b), X1160 (c), X240 (d). Temperatures plotted are the main channel temperature 3 cm, 9 cm and 20 cm depths of the bed sediments.

Conduction Isolation

Figure 2-8 shows a portion of the data collected in the initial bed conduction isolation experiment. The left column (Figure 2-8 (a) – (c)) compares temperatures at the same depth using no cylinder, open cylinder and the fabric capped cylinder. The right column (Figure 2-8 (d) – (f)) compares the temperatures of the different depths for each treatment. As these data all come from the same relative location in the streambed, the boundary conditions are the same, and the sediments are assumed to be of similar make-up. This being the case, it was expected that the sediments would conduct heat in a similar manner. However, as is seen in Figure 2-8, the temperatures observed from the different techniques vary. The open cylinder results in temperatures with higher amplitude and less time lag at all depths than those outside of the cylinder. The fabric capping method has lowest amplitude and greatest time lag at all depths when compared to the other techniques. The discrepancy in results from each isolation method is most likely due to differences in advective flow paths influencing the sediment temperatures.

A second series of data were collected comparing the impermeable aluminum cap to those of the permeable fabric cap. Figure 2-9 shows the temperature time-series from the second conduction isolation experiment from the fall. These data show that in general aluminum is exhibiting the largest decrease in amplitude and increase in time lag with depth. The exception is the 3 cm aluminum capped temperature (Figure 2-9(a)), which has a higher amplitude and smaller time lag than the fabric cap.

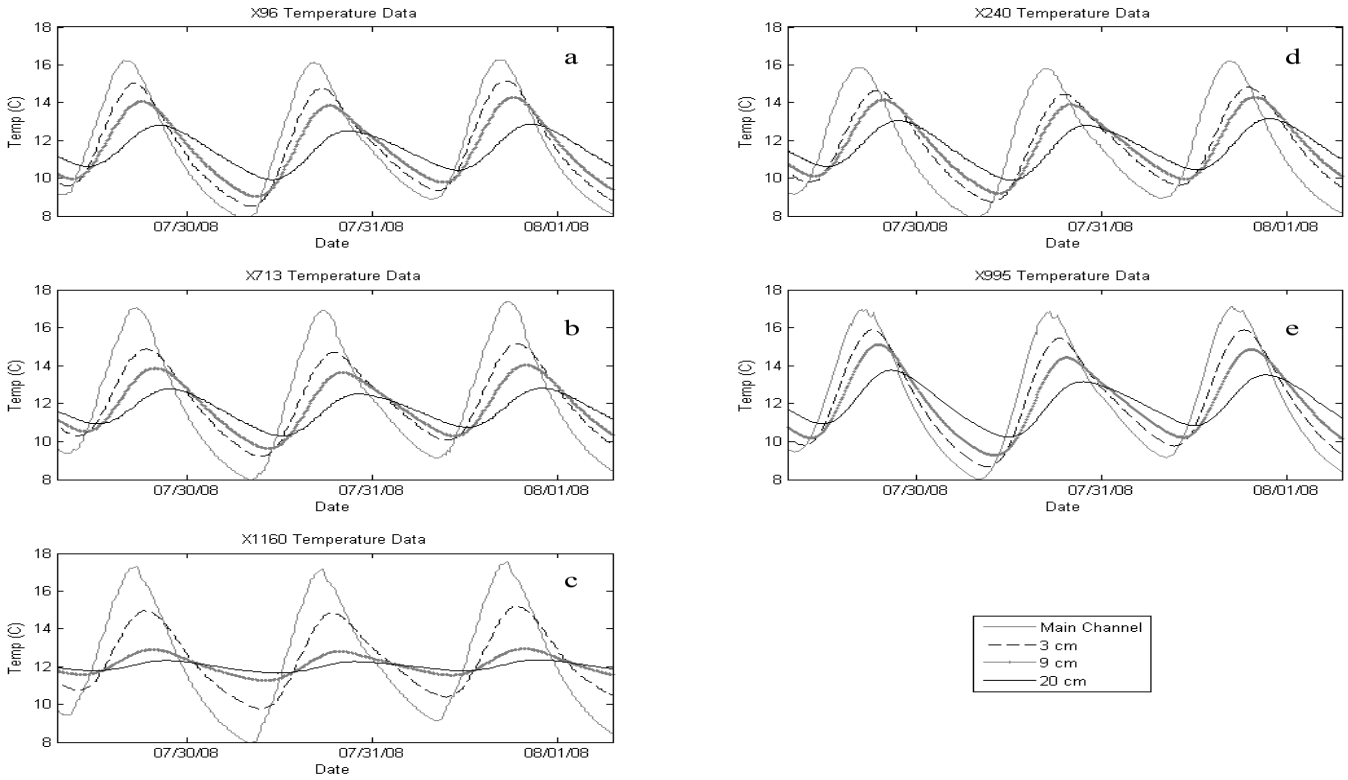

Figure 2-7. Temperature time-series results from Installation Method 2. Cross sections shown X96 (a), X713 (b), X1160 (c), X240 (d), X995 (e). The temperatures shown for each of the locations are the main channel temperature, 3, 9, and 20 cm within the sediment.

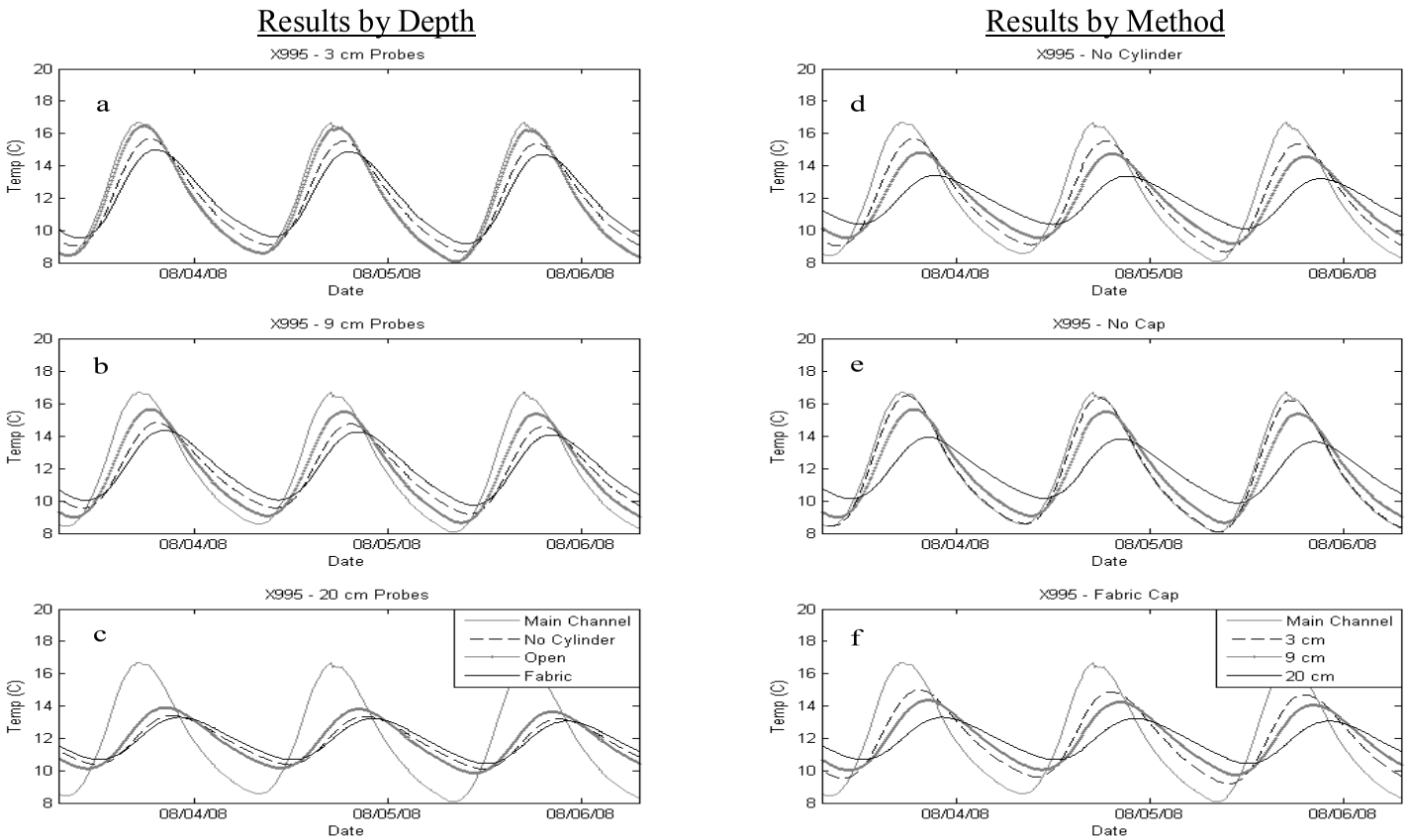

Figure 2-8. X995 Summer Conduction Isolation Experiment. Plots (a) – (c) show different depths of monitoring while different line types denote the isolation technique used. Plots (d) – (f) show the different isolation techniques while different line types show temperatures from monitoring depths.

Sediment Sampling

The sediment samples taken can also be used to help explain the temperature time-series collected. Figure 2-10 shows the composition of the sediment samples taken. Each plot represents a sample location while each of the three lines plotted represents a 7.5 cm section of material removed. These data are plotted on log-log axes where cumulative percentage (i.e., percentage of particles equal to or less than each sieve grid size) is on the Y axis and particle size is along the X axis. These five particle distribution plots show the variability of the sediment size and particle distribution longitudinally as well as with depth. All of the cross sections show larger particles on the sediment surface ("Bed Armor"). Figure 2-10 (a), (b) and (d) show variation of size and distribution with depth while Figure 2-10 (c) and (e) show the two deeper layers of X1160 and X995 to be more homogenous. The data used to create the particle size distributions can be found in Appendix A.

Vertical Head Gradient

In conjunction with the temperature time-series and the particle distributions, vertical hydraulic gradient data were also collected as a means of determining what temperature variations might be due to upwelling or downwelling in the stream (Table 2-2). Five of the sampling sites showed downwelling from the stream while X1160 exhibited upwelling.

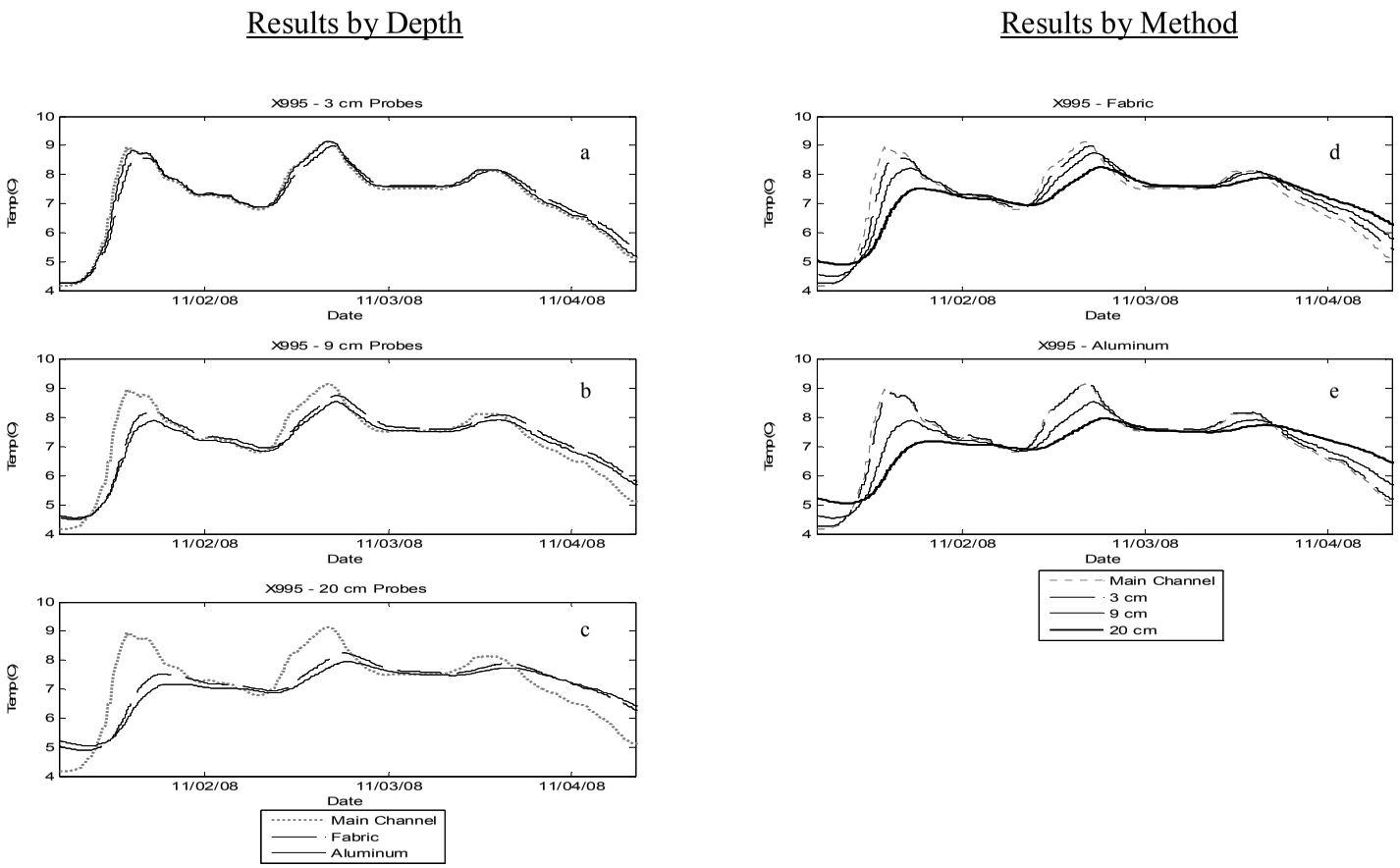

Figure 2-9. X995 Fall Conduction Isolation Experiment. Plots (a) – (c) show temperature at different depths of monitoring while the different line types denote the isolation technique used. Plots (d)– (e) show temperatures from different isolation techniques, different line types show depths of the temperature sensor.

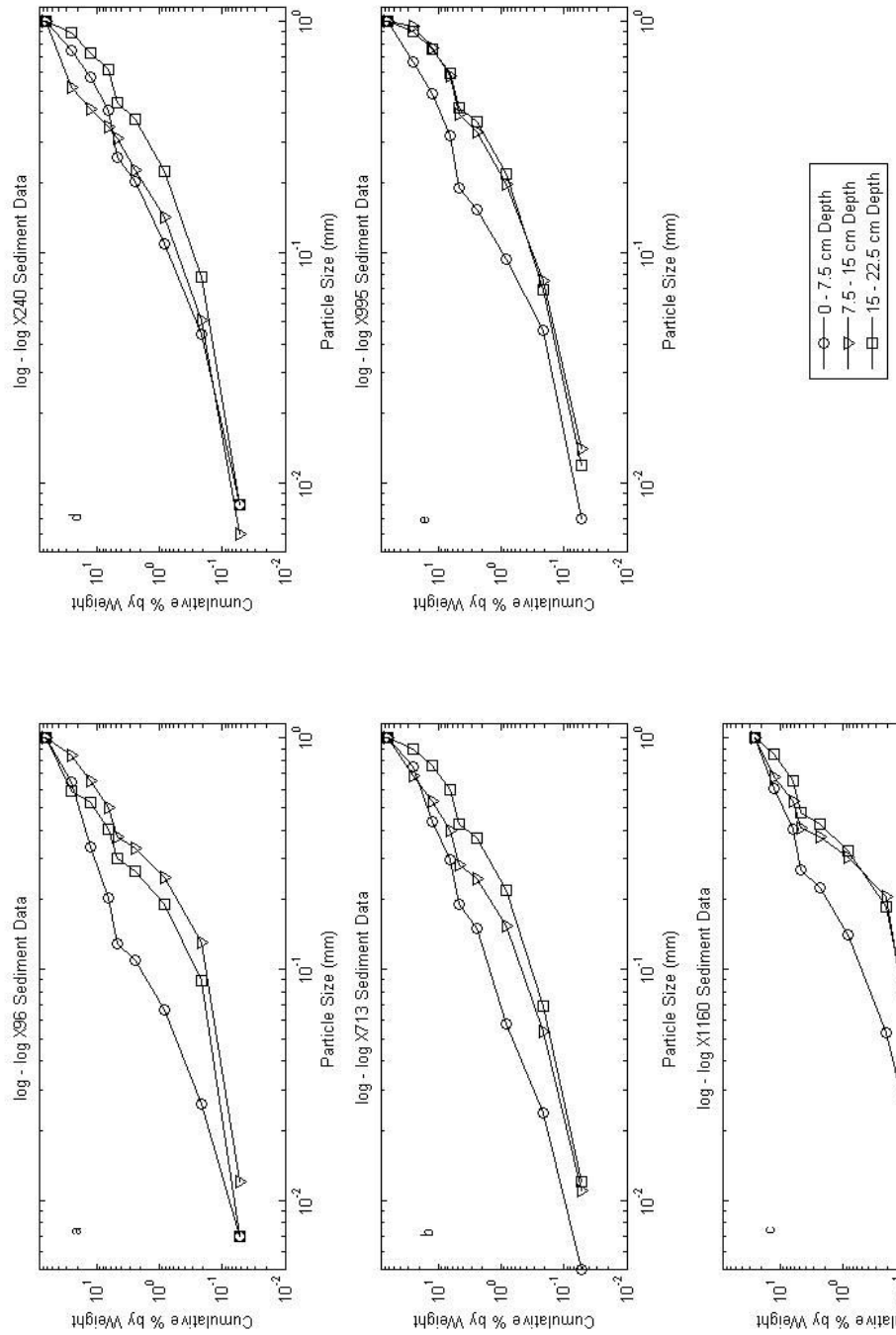

Figure 2-10. Particle size distributions from sediment samples. Each plot shows the particle distribution of the three 7.5 cm layers at each sampling location.

Table 2-2. Vertical Hydraulic Gradient Results. Shows Direction of Flow in or Out of Channel at Cross Sections

Sample Date:	**8/22/2008**	
Location/Depth	9 cm	20 cm
X96	DW	DW
X240	DW	DW
X360	DW	DW
X713	DW	DW
X995	DW	DW
X1160	UW	UW

DW: Denotes downwelling at site
UW: Denotes upwelling at site

Discussion

Each installation and isolation method provides different information regarding the heat fluxes that influence bed sediment temperatures. Since the overarching goal of this study was to compare techniques for installing temperature probe arrays and isolating heating due to bed conduction only, the discussion will primarily focus on identifying the possible shortcomings of each installation and isolation method.

Installation Method 1

Taking a closer look at the results from Installation Method 1, two temperature trends become apparent. Expanding on Figure 2-6 by adding data from more cross sections, Figure 2-11 shows some of the trends resulting from Installation Method 1. The first trend shows sediment temperatures that very closely follow those of the main channel at all depths (Figure 2-11 (a) – (d)). The second trend shows some dampening with increased depth (Figure 2-11 (e) – (f)).

Generally, as the monitoring depth increases, a decreased amplitude and a phase shift is expected in the temperature data [*Constantz*, 2008; *Or et al.*, 2008; *Stonestrom and Blasch*, 2003]. The lack of such differentiation between monitoring depths, and

sediment temperatures tending to those of the main channel suggest that disturbing (digging and burying) the sediments has induced preferential flow from the main channel into the sediment. This is likely due to removing material, losing fine sediments, and replacing it in a more loosely packed manner.

The second trend (Figure 2-11(e) – (f)) of Installation Method 1 shows more of a decrease in amplitude and a phase shift of the temperature data as depth increases. X1160 (Figure 2-11(f)) shows this behavior more than X713 (Figure 2-11(e)). Even so, X713 still exhibits decreased amplitude and a significant phase shift at 20 cm. The reason that these two particular cross-sections differ so much from the other sites can be attributed to the size and distribution of their sediments. The particle distribution (Figure 2-10(b)) indicates that X713's two uppermost sediment layers are composed primarily of larger sediment. The deepest sediment layer shows a greater portion made up of smaller sediment. This may explain the decrease in amplitude and phase shift found in the 20 cm probe. The large sediment of the top layers would repack less densely allowing for water intrusion from the channel. The smaller sediment of the deepest layer would pack more tightly and thus impede more flows through the sediment.

The particle distributions of sediment samples taken from X1160 can also be used to explain some of the temperature trends (Figure 2-10(c)). The change in the distribution between layers is more pronounced in this sampling site. The smaller sediment (< 2.54 cm diameter) goes from approximately 40% in the shallow sediment layer to roughly 50% in the second and about 80% in the third. Just as was hypothesized

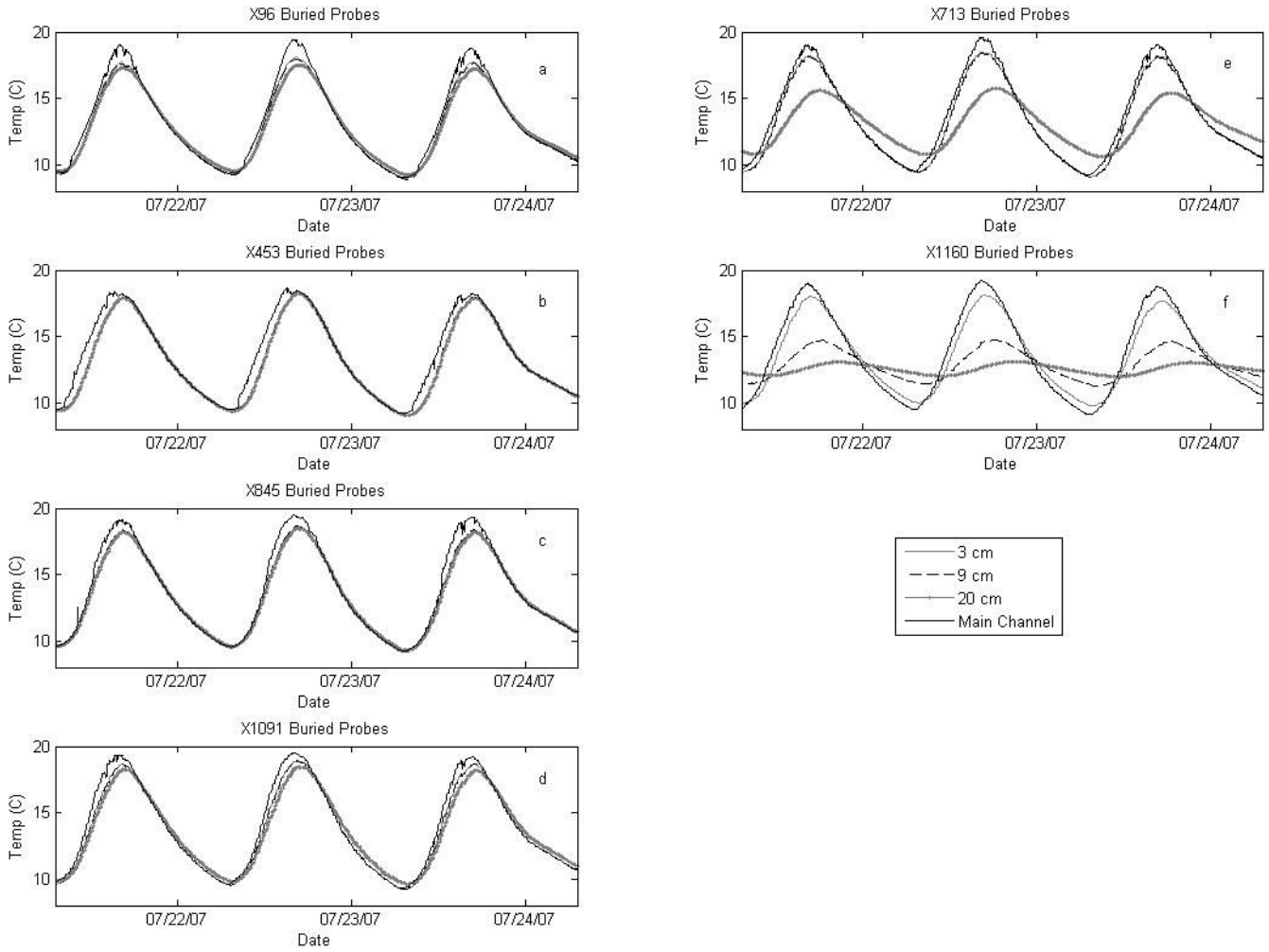

Figure 2-11. Temperature time-series resulting from Installation Method 1. 5(a)-(d) show little temperature variation with depth while 5(e) and (f) show temperature decrease with depth.

in X713, the smaller sediments provide for easier installation, and result in much less disturbance and therefore impeded intrusion. This resulted in the increased dampening and time lag as the sample depth increased.

Installation Method 2

The apparent preferential water flows through the sediment while using Installation Method 1 led to a search for a less intrusive installation method. Installation Method 2 was implemented as an alternative, to compare which of the methods induced the least amount of preferential flow. Figure 2-12 shows a comparison of the methods at two cross sections (X713 and X1160) where both Installation Methods 1 and 2 were applied one year apart. Figure 2-12(a) and (b) show the temperature results from Installation Method 1, while Figure 2-12(c) and (d) show the temperature results from Installation Method 2. Figure 2-12(a) shows a higher temperature amplitude at all three monitoring depths which tends more toward the instream temperature than Figure 2-12(c). Similarly, Figure 2-12(b) differs from Figure 2-12(d) in that the data collected using Installation Method 1 tends more toward the instream temperature. The tendency of the sediment temperatures away from that of the main channel could indicate that Installation Method 2 reduces preferential flow and thus yielding more natural sediment temperature profiles.

Vertical Spatial Temperature Variation

Main channel temperatures are important due to their role in sediment heat fluxes. These temperatures are the boundary condition for both conductive and advective heat flow and spatial variations will cause variations in heat exchange with the bed sediments.

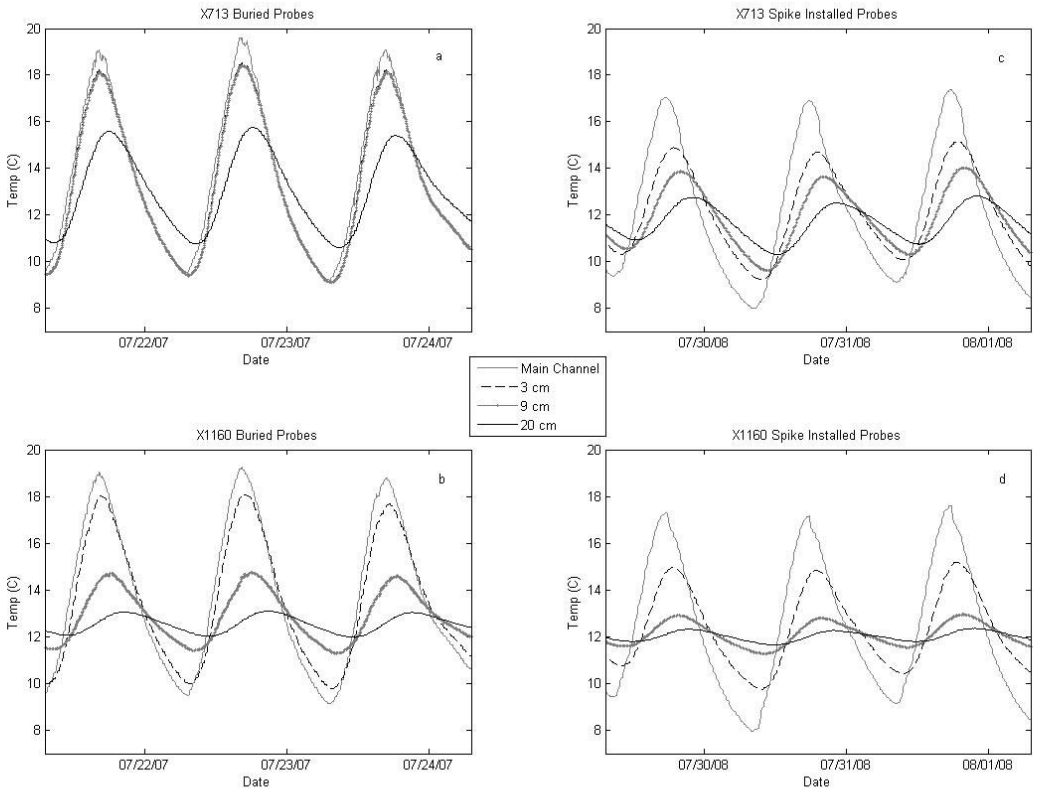

Figure 2-12. Comparison of temperature probe array Installation Methods 1 and 2. Figure 2-12(a) – (b) show Method 1 at X713 and X1160. Figure 2-12(c) – (d) show temperature data collected from the same locations a year later using Installation Method 2.

Figure 2-7 shows temperature time-series from five cross sections that range in position from roughly river meter 100 to 1200 along the study reach. First note the amplitude of the main channel water temperature. Cross sections X96 (Figure 2-7(a)) and X240 (Figure 2-7(b)) only have a maximum temperature of about 16°C while cross sections X713 - X1160 (Figure 2-7 (b), (c) and (e)) nearly reach 17°C. This is likely due to cross sections X96 and X240 being in a segment of the stream where there is more riparian vegetation, resulting in almost complete shading of the stream. At about river meter 450, the trees give way to mostly grasses with intermittent willows resulting in an increase in the amount of solar radiation striking the water surface. Another driver that adds to this

spatial variation is groundwater gains and losses. X96 has a number of groundwater seeps nearby which could also act to cool the main channel during this time of year and in turn the sediments.

Table 2-2 shows that during the sample period, X96 - X995 demonstrated downwelling while X1160 showed a slight upwelling trend. These observations could be used to explain some of the trends in the sediment temperature profiles from the July study. Note that for the most part, the cross sections where downwelling occurred (Figure 2-7(a), (b), (d), and (e)), sediment temperatures have a higher amplitude, similar to that the main channel, which could suggest vertical advection from the main channel into the sediments. X1160 on the other hand, shows a smaller amplitude at the 9 cm depth (Figure 2-7(c)). The 20 cm temperatures show almost a constant temperature of 12.5°C, suggesting that the influences of the stream are no longer significant and the groundwater temperatures dominate. It seems the sensors at these depths are being buffered, which could be due to an input of a lower temperature water. Because of the absence of surface seeps at this location, it would be assumed that this would be due to groundwater upwelling or stream water plunging into the sediments upstream and traveling a long distance before reaching the probes (long hyporheic flow paths). Temperatures observed in the shaded groundwater seeps near X96 and X713 had averages temperature ranging from 10.6 – 10.8ºC which are likely representative of the groundwater temperatures. This supports the hypothesis that the temperatures observed at 20 cm at X1160 is influenced by groundwater.

The difference in the size distribution of sediments at the different monitoring locations is another reason for temperature variation at the different monitoring sites.

Differences in thermal properties can affect heat transfer due to conduction. For example, different sizes of material may vary in density or composition. Additionally, larger substrates can facilitate water exchange due to an increase in porosity which decreases resistance to intrusion of water from the surface or subsurface. Many of the temperature fluctuations described have been due to differing amounts of seepage or advective flows at the different monitoring locations. These advective fluxes, which are commonly present, further underscore the need to isolate temperature effects of bed conduction when collecting data for bed conduction modeling.

Conduction Isolation

Testing of conduction isolation methods was completed at cross section X995 using Installation Method 2 in conjunction with the conduction isolation methods mentioned. In looking at Figure 2-8(a) – (c), each plot shows consistent patterns between each method. First, the highest amplitude temperature is in the main channel followed by the open cylinder. Next is the temperature probe array without a cylinder and finally the fabric capped cylinder. Similar patterns are shown in the time lags. Furthermore, this order is maintained as the depth of the probes increases. However, the amount of temperature variability between the different methods seems to decrease with depth (~ 2 °C at 3 cm of depth and ~ 1°C at 20 cm).

At 3 cm (Figure 2-8(a) and (c)), the open cylinder very closely mimics the main channel temperature and demonstrates the highest amplitude of all the methods at each depth. It was thought that by placing the cylinder around the temperature probe array that the horizontal advective flux would be eliminated and potentially result in temperature variations due primarily to conduction. However, as discussed throughout this study, the

vertical advective exchange with the sediments make this unlikely as the temperature variations in the cylinder are a combined effect of vertical advective exchange and conduction. *Neilson et al.* [2009] found similar results in the Virgin River and stated that higher amplitudes in the cylinder compared to those outside the cylinder are likely due to exclusion of the horizontal flow component through the sediments. The temperature fluctuations of the horizontal flow typically have a smaller diel fluctuation than that of the main channel. When the horizontal and vertical flows are combined (e.g., no cylinder), a smaller amplitude signal may result. The premise of measuring vertical exchange in the cylinders can be further supported by the downwelling found in the vertical hydraulic gradient data for X995 (Table 2-2).

The fabric capped cylinder data exhibited a lower amplitude than the other methods shown in Figure 2-8. It is assumed that this difference is due to the fabric impeding most of the flow that causes advective heat exchange. The unknown amount of exchange being admitted by the fabric is still in question. In preliminary results, *Zhuo* [2009] showed that the fabric cap did limit flows into the sediment, but still admitted about 10%. This suggests that the sediment temperature fluctuations observed by the fabric method would primarily be due to conduction. It was hypothesized that the aluminum cap would better exclude the effects of advection; however, other heat transfer mechanisms could influence this data collection method.

While the data from the aluminum capped cylinder seemed to best represent conductive heating, the way in which the 3 cm aluminum data mimicked the main channel (Figure 2-9(a) and (e)) raises questions regarding this method. It is expected that the aluminum data would result in a decrease in amplitude and a phase shift at this depth

in excess of the fabric data. However, the opposite occurs. X995 is exposed to direct sunlight most of the day and during the fall, only 5 – 7.5 cm of water covers these capped cylinders. It is possible that the aluminum cap is being heated due to solar radiation penetrating the water column and consequently increasing the rate of conduction in the shallow sediments. Based on the trends shown at the different depths, another possibility is a clerical error where the 3 cm fabric probe was switched with the 3 cm aluminum probe. As a test, it is recommended that this technique be applied at X995 during the summer and at a shaded location such as X240 to see if this trend manifests itself again.

It is interesting to note the shift that can be seen from November 3rd to the 4th (Figure 2-9). This was the transition from fall temperatures to winter. We see that the main channel goes from being the warmest to the coldest and the 20 cm depth goes from being the heat sink to being the heat source. For use of these data in conventional conduction modeling applications, it would be recommended that the data collection take place during consistent conditions rather than transition periods.

Conclusions

Data were collected on Curtis Creek to identify the sediment temperature monitoring methods that represent heating due to conduction. Of the installation techniques for the sediment temperature probe arrays, Installation Method 2 (spike installation technique) yielded the results that induced the least amount of preferential flow. It was adopted in the subsequent data collection stages and is recommended as the best practice for monitoring in situ sediment temperature variation due to both hyporheic exchange and bed conduction.

To isolate temperature variability due to conduction, temperature probe arrays installed using this method were surrounded by a steel cylinder and topped with two different capping materials. While the fabric capping technique yielded results less influenced by advection than the open cylinder technique used previously by *Neilson et al.* [2009], it still permitted some advective flow through the cylinder which may affect its use in the conduction modeling. The aluminum capping technique is the only technique explored in this research that did indeed limit all advective flow from the channel; however, the results may have been influenced by heating due to solar radiation. Further research is recommended to test the theory of heating by solar radiation. The data collected from the sediment sampling and vertical hydraulic gradients yielded data that proved to aid in interpreting the sediment temperature results.

CHAPTER 3

COMPARISON OF METHODS FOR THE DETERMATION OF STREAMBED THERMAL PROPERTIES

Abstract

Sediment thermal properties are vital to an accurate approximation of many stream characteristics such as future instream temperature and groundwater seepage. When approximating them, values from literature or results from mixture and calibrated conduction models are typically used. To determine which approach yields the most representative results, this research compares the use of both mixture and the bed conduction model SEDMOD to estimate thermal conductivity and diffusivity while investigating the supporting data collection techniques. Mixture models estimate overall thermal conductivity and were populated by combining data from sediment samples with literature thermal property values. Different methods of collecting streambed sediment temperature profiles were used with SEDMOD to 1) estimate thermal diffusivity and 2) use the thermal diffusivity results to determine which data collection methods better represent conductive heating only. The data collection methods covered different techniques of isolating temperature probe arrays from advective influences by using a steel cylinder and caps of different materials. The resulting thermal diffusivity values were then compared to laboratory measurements in order to determine the most representative method. It was found that a volume weighted averaging technique was the most accurate mixture model applied. SEDMOD best approximated streambed

properties using data collected in a steel cylinder with an aluminum cap to isolate the temperature probe array.

Introduction

Stream temperature is a topic of study and interest primarily due to its effects on water chemistry, growth, development and life cycles of fish and other aquatic life [*Allen*, 1995]. It has also been found to influence the rate at which water leaves the stream through groundwater infiltration or seepage [*Ronan et al.*, 1998]. Using heat as a tracer, many studies estimate seepage rates in streambeds using temperature data collected in the bed sediments [*Constantz*, 1998, 2008; *Hatch et al.*, 2006; *Ronan et al.*, 1998; *USGS*, 2003].

Stream temperature models have been constructed to understand the dominant processes influencing instream temperature [*Chapra et al.*, 2004; *Evans et al.*, 1998; *Healy and Ronan*, 2003; *Morse*, 1970; *Neilson*, 2006; *Sinokrot and Stefan*, 1993, 1994] and thus provide a tool for managing water resources. One weak point of these seepage and temperature modeling efforts is the need to assign thermal properties to the sediments in order to quantify the rates of bed conduction (heat transfer due to a temperature gradient across medium). Many use literature values for thermal conductivity (k), bulk density (ρ_b), heat capacity (C_p), and thermal diffusivity (α) [*Chapra et al.*, 2004; *Evans et al.*, 1998; *Hatch et al.*, 2006; *Jobson*, 1977; *Morse*, 1970; *Sinokrot and Stefan*, 1994; *Stonestrom and Blasch*, 2003]. These studies make a general estimate of the bed make up (i.e., rock, limestone, sand, etc.) and literature values are applied accordingly. The concern with this practice is that the literature values usually only give a general

description of the material (such as a common name) which leaves one to guess which of the materials match the streambed being studied.

Another method of estimating thermal properties of sediment is through the use of mixture models. Generally these models are used by soil scientists to estimate the overall thermal properties of a soil mixture [*Campbell*, 1985; *Tindall et al.*, 1999; *Zang et al.*, 2007], however, similar methods have also been applied in stream temperature modeling [*Boyd and Kasper*, 2003]. Mixture models are relationships designed to calculate the overall thermal properties of a heterogeneous media based on soil or sediment properties.

To estimate more site specific thermal properties, many have collected sediment temperature profiles and used a heat conduction model to estimate the thermal properties of the bed [*Chapra*, 2005; *Hondzo and Stefan*, 1994; *Ronan et al.*, 1998; *Sinokrot and Stefan*, 1993]. These models are typically based on the conduction equation. The advantage to applying these models is the use of site specific sediment temperature profiles to estimate thermal properties through model calibration. A shortfall of this method is the assumption that the data collected represent the effects of bed conduction only. Many insert temperature probe arrays into the stream sediments and assume that temperature dynamics are due only to conduction. It is possible that these measurements represent a combination of advection and conduction which are generally dominant in the streambed [*Constantz*, 2008; *Neilson et al.*, 2009].

While these methods are commonly applied throughout literature, a literature review for this research showed no evidence of a comparison of methods to determine which of these parameter estimation techniques most accurately approximates the conduction properties of the streambed. Towards this end, this research compares the

results of some commonly used mixture models and the conduction model SEDMOD, in order to recommend the method that best approximates conduction parameters. To provide an absolute measure, sediment samples were sent to a thermal properties laboratory. As the approach to collecting sediment temperature data can drastically affect the ability to estimate the thermal properties of the streambed, sediment temperature monitoring techniques for isolation of bed conduction were additionally tested and will be discussed.

Site Description

The stream selected for this research was Curtis Creek in Northern Utah, on the Hardware Ranch Wildlife Management Area. The location of the ranch is about 24 kilometers east of the City of Hyrum in Cache County, Utah (Figure 3-1). The property is owned by the State of Utah and is used as wildlife habitat and a winter feeding ground for the local Rocky Mountain Elk population. Prior to the state acquiring the land, the property had several owners, mostly made up of homesteaders or ranchers [*Christensen*, 2007]. Anthropogenic use of stream water is currently limited to stock watering and flood irrigation. In recent history, the State of Utah used federal grant money for a stream relocation project that moved a section of the creek away from their animal corrals [*Division of Wildlife Resources*, 2001]. The river reach considered in this study is about 1.5 km in length, stretching roughly from Laketown Road to state Highway 101 (Figure 3-1).

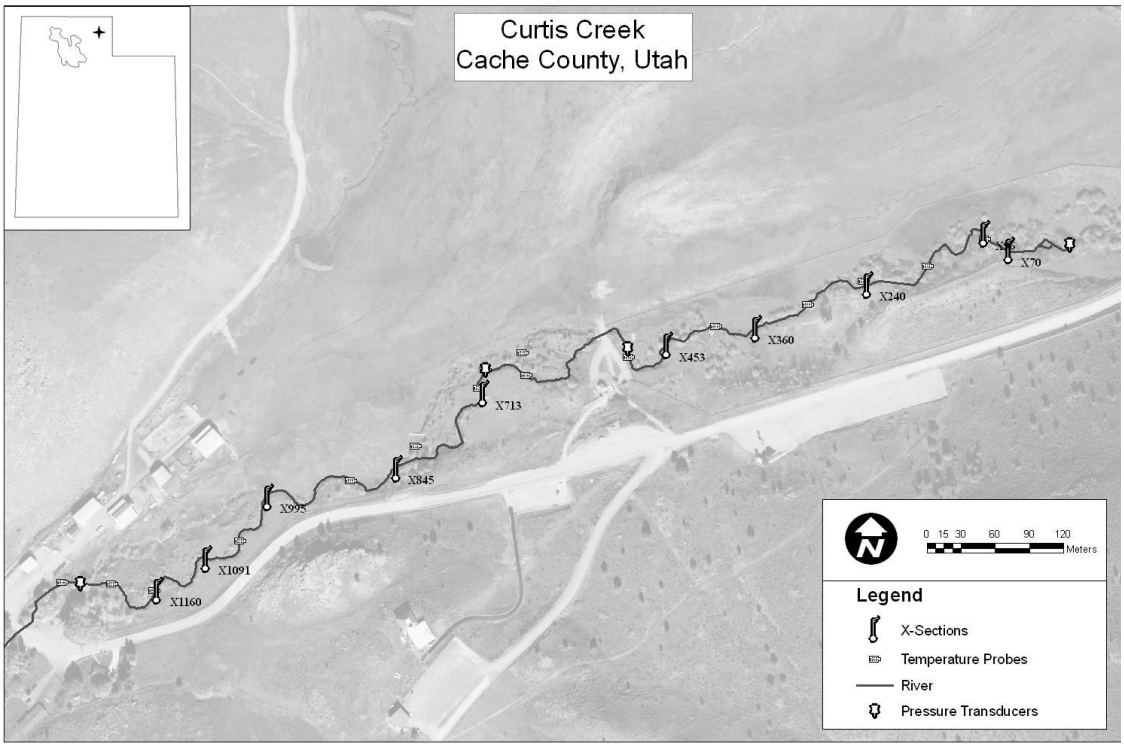

Figure 3-1. Study reach at Curtis Creek, Utah, showing data sampling locations.

Curtis Creek is a high gradient mountain stream with an average bed slope of 2% and an average bankfull width of 3.7 m. The bed material of the stream consists of mostly gravel and cobble sized rock (2 - 15 cm diameter). The study reach is highly influenced by groundwater, consisting of both groundwater/surface water interactions as well as overland flow from surface seeps to the stream.

Ten data collection locations (referred to as "cross sections") were selected where instream temperatures were monitored as well as sediment and vertical hydraulic gradient data collected. Figure 3-1 shows the distribution of these cross sections. The data collection sites are designated by their position downstream from the uppermost flow gauge (i.e., X1160 is the cross section found 1160 meters downstream of the uppermost gauging station of the research reach).

Of all of the data collection sites along the study reach, X995 was selected as a site to compare conduction isolation and parameter estimation methods. X995 was selected because its substrate was similar to the other observation sites, but not large enough to prevent two steel isolation cylinders from being installed into the streambed for the comparison of methods.

Laboratory Methods

In order to have a standard estimate of the actual thermal properties of the sediment, three layers of bed sediments from X995 were sent to the Thermophysical Properties Research Laboratory (West Lafayette, IN). The sediments were analyzed for thermal conductivity as well as specific heat capacity. A heated probe method [*ASTM*, 2008] was used to measure the thermal conductivity of the three saturated samples. Three readings were taken per sample in order to calculate an average thermal conductivity for each layer. Three sediment sizes were selected for measurement of specific heat capacity (6.35 cm, 0.64 cm, and 0.02 cm). A differential scanning calorimeter was used with sapphire as the reference material to measure specific heat capacity [*ASTM*, 2005]. Larger sediments were broken into smaller (< 1 cm diameter) pieces in order to fit into the calorimeter.

Field Data Collection Methods

Sediment Sampling

The data collected at cross section X995 included both physical sediment samples and sediment temperature time-series. To define the sample volume, sediment samples

were taken by inserting a 30 cm diameter stainless steel cylinder into the streambed to a depth of 22.5 cm. The resulting sediment core was removed in three layers at depths of 0 - 7.5 cm, 7.5 – 15 cm, and 15 - 22.5 cm. This allowed the sediments to be stored in 2 gallon buckets for transport. The samples were separated into different size fractions through sieving. The size fractions were weighed using a Mettler Toledo® PL6001-S scale (Columbus, OH) and volumes were measured by submerging each fraction in water and noting the volume of water displaced. Bulk density of the sediment was calculated using the sediment mass and volume measurements by taking the sum of the weight divided by the sum of the sediment volume for each of the samples (Equation 3-1).

$$\frac{\sum_{i=1}^{n} Mass_i}{\sum_{i=1}^{n} Volume_i} = \rho_b \qquad (3\text{-}1)$$

n = number of size fractions in the sediment sample. The volume of water in the interstices of the sediment was calculated by subtracting the sum of the sediment volumes from the total sample volume. After weighing and measuring the volumes of the sediment sample, the mineral composition of the rocks was identified. The larger substrate (> 0.64 cm) consisted of mostly lime mudstone, followed by small amounts of dolomite, sandstone, and quartz. The sands were made up mostly of quartz mixed with traces of chert, calcite, dolomite and organic matter [*D. Lidell*, personal communication February 11, 2009].

Sediment Temperature Data

In order to estimate the thermal diffusivity of the bed sediments using SEDMOD, sediment temperature time-series needed to be collected. HOBO® Temp Pro V2 temperature probes (Onset Computer Corporation, Bourne, MA) were installed at 3, 9, and 20 cm below the streambed surface (referred to as "temperature probe arrays" throughout). These temperature probe arrays were installed using a spike and sleeve technique similar to other applications [*Baxter and Hauer*, 2003; *Constantz et al.*, 2002; *Stonestrom and Blasch*, 2003]. A second data collection technique was used to attempt to isolate heating due to bed conduction only. Thirty centimeter diameter steel cylinders were driven into the streambed to a depth of 30 cm to impede lateral advective flow from influencing the temperature probe arrays that were installed in the center of the cylinder. Different methods of impeding advective flow through the cylinder were tested: no isolation cylinder, an open top cylinder, a cylinder with a geo-fabric cap, and a cylinder with an aluminum cap. A more detailed description of these data collection methods and capping techniques can be found in Chapter 2.

During the summer 2008 deployment, one temperature probe array was placed in the streambed at X995 without an isolation cylinder. Two cylinders were also installed at X995 with temperature probe arrays installed within them. During the summer, one cylinder had an open top and one had a geo-fabric cap. In the fall, a similar test was performed, with the difference being that one cylinder was capped with geo-fabric while the other was capped with a thin aluminum covering.

Modeling Methods

The models used in this research have been selected because of their wide use and ability to approximate site specific thermal properties rather than using assumed values. These models can be divided into two different groups, mixture models and a conduction model. The mixture models used in this research use volumes of the mixture constituents or sediment density as well as literature thermal properties to calculate overall thermal conductivity for a heterogeneous mixture. Temperature time-series were collected at different depths within the sediment in order to calibrate SEDMOD. This model estimates thermal diffusivity by altering this variable in order to match the observed sediment temperatures.

In order for the thermal conductivities from the laboratory and the various mixture models to be converted to thermal diffusivity, Equation 3-2 was used [*Incropera et al.*, 2007; *Stonestrom and Blasch*, 2003]. The conversion of thermal conductivity into thermal diffusivity will allow for a direct comparison between the laboratory, mixture model and conduction model results.

$$\alpha = \frac{k_{total}}{\rho_t \cdot C_p} = \frac{k_{total}}{C_v} \tag{3-2}$$

α = thermal diffusivity (cm^2/s), ρ_t = density of sediment mix (both sediment and water) (g/cm^3), C_p = specific heat capacity ($J/(g\ °C)$), and C_v = volumetric heat capacity ($J/(cm^3\ °C)$). To make the conversion to thermal diffusivity, volumetric heat capacity was calculated using Equation 3-3 [*Constantz et al.*, 2002; *DeVries*, 1963; *Or et al.*,

2008; *Stonestrom and Blasch*, 2003]. Bulk density of the sediments (ρ_b) was calculated from sediment sample information using Equation 3-1. Density of water (ρ_{water}), and specific heats (C_p) of both water and sediment come from laboratory measurements or literature.

$$C_v = \sum_{i=1}^{n}\left[\rho_b \cdot C_{p_{sed}} \cdot \frac{V_{sed}}{V_{total}}\right]_i + \rho_{water} \cdot C_{p_{water}} \cdot \frac{V_{water}}{V_{total}} \tag{3-3}$$

V_{sed} = volume of the sediment fraction (cm^3), V_{sand} = volume of the smaller sediments (cm^3), V_{water} = volume of water in sample (cm^3), and V_{total} = total volume of sample (cm^3).

Mixture Models

The heterogeneity of the streambed casts doubt on the practice of assigning one literature value to the streambed as a whole. However, the use of mixture models to approximate the effects of a sediment mix may provide a better estimate of the thermal properties of the streambed. Based on the mineral composition, thermal conductivity values can be assigned from literature. In Curtis Creek, gravel and cobble (6.35 cm – 0.24 cm sieve size) sediments were primarily composed of limestone, and were thus assumed to have a thermal conductivity of 2.15 W/(m ºC) [*Incropera et al.*, 2007], smaller sands (0.08 cm and smaller) were assigned the thermal conductivity of sand (2.5 W/(m ºC)) [*Andrews and Rodvey*, 1980] and water, the thermal conductivity of water (0.058 W/(m ºC)) [*Bejan*, 1993; *Cengel*, 1998; *Grigull and Sandner*, 1984; *Mills*, 1992].

The first mixture model selected for comparison was that used by *Boyd and Kasper* [2003], which implements a volumetric composite approach (Equation 3-4). In

this approach, the thermal property of each constituent is multiplied by its fraction of the total sample volume. The constituents considered were sediment, water, and air. This research expands on this assumption by dividing the volume fraction into larger stone substrate, smaller sands, and water. The fraction of air present in the streambed was considered to be negligible.

$$k_{total} = k_{rock}\frac{V_{rock}}{V_{total}} + k_{sand}\frac{V_{sand}}{V_{total}} + k_{water}\frac{V_{water}}{V_{total}} \tag{3-4}$$

V_{rock} = volume of the larger sediments (cm^3), V_{sand} = volume of the smaller sediments (cm^3), V_{water} = volume of water in sample (cm^3), V_{total} = total volume of sample (cm^3), k_{rock} = thermal conductivity of large sediments (W/(cm °C)), k_{sand} = thermal conductivity of smaller sediments (W/(cm °C)), k_{water} = thermal conductivity of water (W/(cm °C)), and k_{total} = total thermal conductivity of total sample (W/(cm °C)).

The second mixture model used in this research was proposed by *Zang* [2007]. Zang's method is based on the porosity and saturation of the sample (Equation 3-5).

$$k_{total} = \left[(1-\phi)k_{sed}^{\frac{1}{2}} + \phi \cdot S \cdot k_{water}^{\frac{1}{2}}\right]^2 \tag{3-5}$$

Φ = Porosity (dimensionless), and S = saturation (dimensionless). Equation 3-5 can be simplified to Equation 3-6 using the definition of porosity (ratio of the fluid volume to the total volume) and assuming complete saturation (all void space filled with

water). Due to the inability of the model to account for more types of sediment, the thermal conductivity of the most common substrate (limestone) was applied.

$$k_{total} = \left[k_{sed}^{\frac{1}{2}} \frac{V_{rock}}{V_{total}} + k_{water}^{\frac{1}{2}} \frac{V_{water}}{V_{total}} \right]^2 \tag{3-6}$$

The final mixture model used is that proposed by *Campbell* [1985]. Campbell's relationship does not use volume, porosity or even thermal conductivity as do the other equations. Rather, this equation is based on an empirical relationship of bulk density and volumetric water content (ratio of water volume to total volume) of the sample (Equation 3-7).

$$\begin{aligned} k_{total} &= A + B\theta_v \\ A &= 0.65 - 0.78\rho_b + 0.6\rho_b^2 \\ B &= 1.06\rho_b \end{aligned} \tag{3-7}$$

ρ_b = bulk density of the sample (g/cm^3) and θ_v = volumetric water content of sample (dimensionless). A table of the volumes and densities used in this section can be found in Appendix B.

Unfortunately, none of the authors of these mixture models state the amount of error associated with the predictions using their methods. Due to this lack of information a statistical comparison was not attempted. Rather, the models will be compared based on their ability to approximate the thermal conductivity and diffusivity values similar to those measured by the laboratory.

Conduction Model

The conduction model applied was the sediment heat transfer model SEDMOD (Dr. Steven Chapra, Medford, MA). SEDMOD uses a numerical approximation of the Heat Conduction Equation to estimate conduction through the sediments (Equation 3-8).

$$\frac{\partial T}{\partial t} = \alpha \frac{\partial^2 T}{\partial z^2} \tag{3-8}$$

T = temperature (°C), t = time (seconds), z = depth (cm), and α = thermal diffusivity (cm^2/s). Heat is assumed to be transferred through the streambed, assuming a semi-infinite slab (Figure 3-2). This approach produces a thermal diffusivity for the entire slab to the depth modeled. In this research a 1m depth was set as the bottom boundary.

In its original form, main channel temperatures are applied as a top boundary condition (T_0 at Z_0) and a bottom boundary is approximated as the average of the main channel temperature. Model results are plotted and compared to the observed sediment temperatures at their respective depths (e.g., $T_{3,\ observed}$ at Z_3 is compared to $T_{3,\ modeled}$ at Z_3). Thermal diffusivity is adjusted in an effort to match the model output to the observed sediment temperature profile.

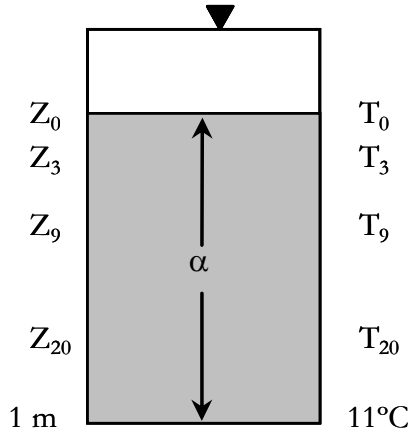

Figure 3-2. SEDMOD model schematic with the final bottom boundaries applied.

To expand on this approach a number of changes were made to the SEDMOD code. First, the trial and error graphical calibration of the model was too subjective for comparison purposes. Computer code was added to the model that would initially run the model with a thermal diffusivity value of 0.0001 cm^2/s. Upon completion the model would rerun after incrementing 0.0001 cm^2/s. This would continue until reaching a predetermined stopping point of 0.05 cm^2/s. The residual sum of squares (RSS) [*Berthouex and Brown*, 2002] between the model results and corresponding observed temperatures was calculated for each incremental thermal diffusivity value. These RSS results (at 3 cm, 9 cm, and 20 cm) were summed and the point at which this overall RSS value was minimized (least sum of squares) was considered the best estimate of thermal diffusivity for each isolation technique used.

In collaboration with Dr. Steven Chapra, SEDMOD was further altered to be able to establish a fixed bottom boundary temperature. Along with this adaptation, code was added to facilitate the setting of initial temperatures at various sediment monitoring depths rather than the averaged main channel estimate previously used.

For each simulation, the observed temperatures at the beginning of the simulation time period and their respective sediment depths were used to initialize the model. Along with initializing the model with these observed sediment temperatures it was necessary to set a bottom boundary temperature (temperature at 1m depth). Water temperatures from shallow groundwater observation wells were measured to assist in setting the bottom boundary condition, but they yielded erratic results ranging from 16 – 18ºC. These observations were likely not representative as fall sediment temperatures at 20 cm ranged from 3 – 7°C. This observation indicates that the well water may have been influenced by its exposure to the atmosphere or that the brown sample bottles were heated by the sun prior to measurement. Comparing these temperatures to groundwater temperatures from other research, these temperatures appear much too high [*Constantz*, 1998; *Constantz et al.*, 2002; *Lee and Hahn*, 2006]. As another approach to approximating the bottom boundary condition, close attention was paid to X1160 where groundwater upwelling was observed. The temperature data collected at the 20 cm depth in the sediments of X1160 showed little variation from the average temperature of 12.5ºC. The temperature of the groundwater seeps at X96 and X713 showed average temperatures ranging from 10.6 – 10.7ºC. Considering the well, seep, sediment temperature, and literature information, the bottom boundary temperature was set to be 11ºC at a 1 meter depth.

The diffusivity and RSS outputs of SEDMOD lend themselves to the use of a critical sum of squares analysis to determine confidence bounds of each simulation [*Berthouex and Brown*, 2002] (Equation 3-9).

$$S_c = S_R + S_R \cdot \left(\frac{p}{n-p} \cdot F_{P,n-p,\alpha} \right) \tag{3-9}$$

S_c = critical sum of squares value, S_R = least sum of squares value, p = number of parameters estimated, n = data points collected, and $F_{p,n-p,\alpha}$ = F distribution (upper 5%). Thermal diffusivity results are plotted against their respective RSS values, and the confidence bounds are taken as the X axis values where the critical sum of squares value intersects the resulting curve. These statistical calculations can be found in Appendix C. Residual plots were also made of the simulation results by plotting the residuals against measurement depth. The residual plots can be found in Appendix D.

Results

Laboratory Results

Table 3-1 shows the laboratory measurements for specific heat capacity for the three size fractions analyzed at various temperatures. Only the values applicable to this research (10-30°C) are included. Though small, there are differences in the specific heat capacity at different temperatures.

Table 3-2 shows the laboratory results for thermal conductivity at 19°C for the three sediment depths sampled. Triplicate measurements were taken for each sample. The table shows the average of the three measurements as well as a standard deviation. The second sediment layer has a lower thermal conductivity than the other two layers.

Table 3-1. Specific Heat Capacity Results from Lab Analysis. Shows the Three Sizes of Material Measured and the Temperature at Which the Reading Was Taken

T/C	Cp/(J/g C)		
	#70	1/4"	2 1/2"
10	0.737	0.796	0.773
20	0.771	0.833	0.800
30	0.797	0.863	0.824

Table 3-2. Thermal Conductivity Results from Lab Analysis. Thermal Conductivity Was Measured at 19°C. The Results of the Measurements Are Shown for Each Sediment Layer. An Average Value by Layer and Standard Deviation Is Also Included

		k/(W/m C) X995	
T/C	**0 - 7.5 cm**	**7.5 - 15 cm**	**15 - 22.5 cm**
19	1.748	1.563	1.802
19	1.854	1.554	1.833
19	1.876	1.564	1.832
Average	**1.826**	**1.560**	**1.822**
STDEV	0.068	0.006	0.018

To be consistent with the temperature at which the thermal conductivity measurements were made, the specific heat values were interpolated to a temperature of 19°C. As there were only three size fractions for which specific heat values were measured by the laboratory, these were applied in three size ranges; 1.27 – 6.35 cm sediment (0.793 J/(g °C)), 0.24 – 0.64 cm sediment (0.8293 J/(g °C)), and 0.08 – 0.005 cm sediment (0.7676 J/(g °C)). Using these specific heat values with the bulk densities calculated using the sediment samples, volumetric heat capacity values were estimated for each sediment layer and for all three layers combined. A summary of the thermal properties by layer can be found in Table 3-3.

The average thermal conductivity value from the combined laboratory results was divided by the overall volumetric heat capacity for the whole streambed, giving an overall thermal diffusivity of 0.0068 cm^2/s.

Table 3-3. Thermal Properties for Each Sediment Layer Based on the Thermal Conductivities and Specific Heats Measured in the Laboratory As Well As Calculated Bulk Densities of Each Layer. The Properties Shown Are Thermal Conductivity, Volumetric Heat Capacity, and Thermal Diffusivity for Each Sediment Layer

	X995		
	0 - 7.5 cm	**7.5 - 15 cm**	**15 - 22.5 cm**
k (W/(m ºC))	1.83	1.56	1.82
C_v (J/(cm^3 ºC))	2.42	2.62	2.60
α (cm^2/s)	0.0075	0.0059	0.0070

Field Data Results

Figure 3-3 shows a log-log plot of the particle size distribution by weight for X995. The graph is a cumulative size distribution where each data point represents the percentage of material in the sample of a given size and smaller. For example, the 0 – 7.5 cm depth shows that 66% of the material of that layer is 2.5 cm in diameter or less. The three line types represent the three sampling depths (0-7.5 cm, 7.5-15 cm, 15-22.5 cm). Note that the top sediment layer is larger than the two subsequent layers which are very similar to each other in size and distribution.

To isolate the effects of bed conduction, temperature time-series were collected in various ways, these data were used as calibration data for SEDMOD. Figure 3-4 shows the temperature time-series data collected using no isolation cylinder, an open cylinder, and the fabric capped cylinder for the summer of 2008. The data have been plotted by depth (Figure 3-4 (a) – (c)) and by method (Figure 3-4 (d) – (f)). Notice the decrease in temperature amplitude as depth increases among the methods used. The amplitude decrease with depth is expected, but the decrease in temperature amplitude between different methods at the same depth is likely to be due to a decrease in advective flow.

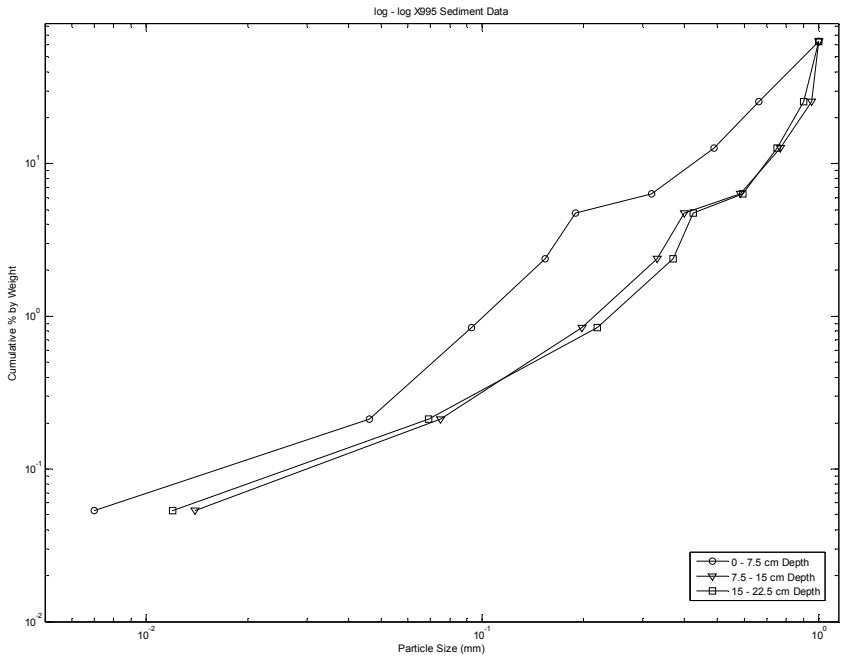

Figure 3-3. Log-log sediment particle distribution for X995. Three line types shown represent each sediment layer sampled. Plot shows a stark difference between the size and distribution of the first sediment layer in reference to the others.

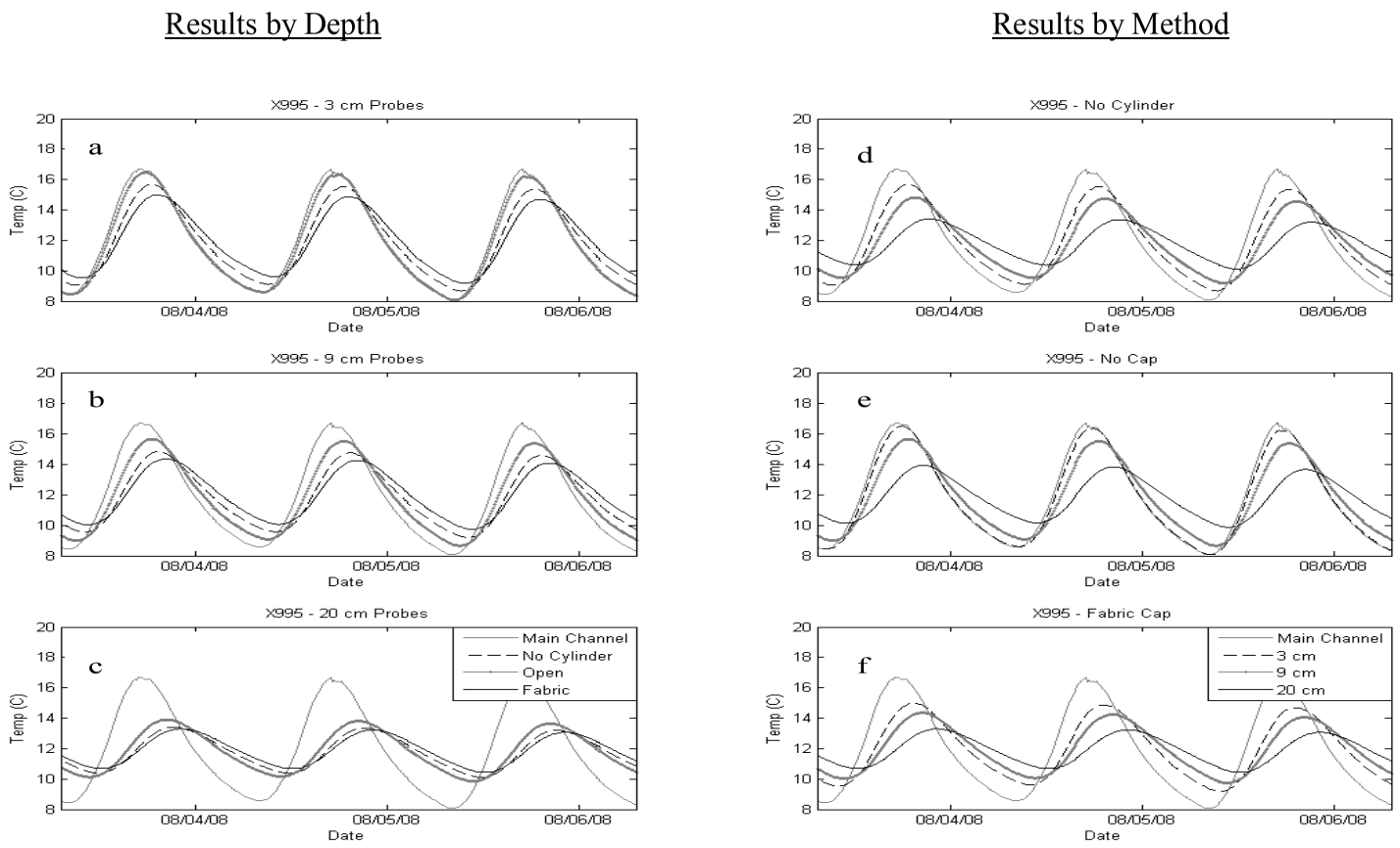

Figure 3-4. Temperature time-series from no cylinder, open cylinder, and fabric capped cylinder. Figure 3-4(a) – (c) show a comparison of the different methods by depth of installation. Figure 3-4(d) – (f) plots the different depths by method.

Figure 3-5 shows the temperature time-series resulting from the Fall 2008 experiment where the aluminum cap, fabric cap, and no cylinder methods of isolating conductive heating were tested. Figure 3-5(a) – (c) plots the different monitoring depths and Figure 3-5(d) – (f) plots the different isolation methods. This data taken in the fall is much more compressed than in the summer. Better model estimations may result if the data were more consistent as in Figure 3-4. Even so, a temperature dampening with depth can be seen between the isolation methods used.

Modeling Results

Using the volumes measured from the sediment samples, porosity and volumetric water content were calculated. This data was used with the measured densities to estimate total thermal conductivities for the three sediment depths using the three mixture models mentioned. Table 3-4 shows the results of the mixture models used in this research.

Thermal diffusivities were calculated for each sediment layer by dividing the thermal conductivities from Table 3-4 by their respective volumetric heat capacities. The overall thermal conductivity for the streambed was calculated by applying the mixture models to the entire sediment core. The results were then divided by the overall volumetric heat capacity (Equation 3-7) of 2.5508 J/(cm^3 °C) to determine the overall thermal diffusivity of each mixture model (Table 3-5). For ease of notation, the diffusivities have been labeled by the monitoring depth they represent (e.g., α_3 represents sediment layer from 0-3 cm, α represents overall diffusivity of the bed). The accuracy of the thermal diffusivity calculations closely followed the accuracy of the model in approximating thermal conductivity. This conversion of thermal conductivity from the

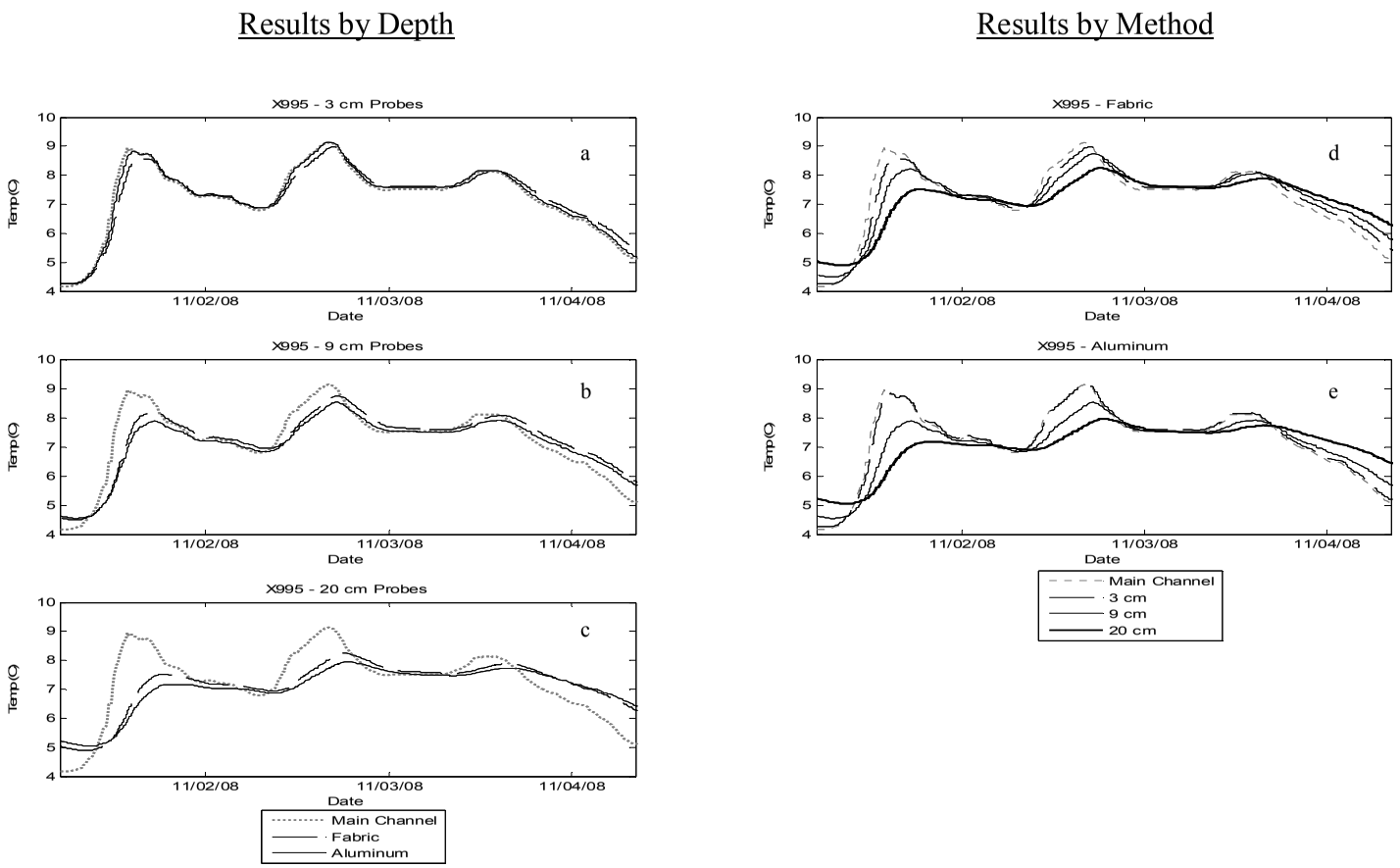

Figure 3-5. Temperature time-series from no cylinder, fabric capped cylinder, and aluminum capped cylinder. Figure 3-5 (a) – (c) show a comparison of the different methods by depth of installation. Figure 3-5 (d) – (e) plots the different depths by method.

Table 3-4. Thermal Conductivity Results Using the Three Mixture Models. Thermal Conductivity Results by Sediment Layer for Each of the Mixture Models Compared to the Measured Laboratory Values

Depth	Volume Ave k (W/(m ºC))	Zang k (W/(m ºC))	Campbell k (W/(m ºC))	Lab k (W/(m ºC))
0 - 7.5 cm	1.81	1.56	3.38	1.83
7.5 - 15 cm	1.69	1.36	3.93	1.56
15 - 22.5 cm	1.71	1.37	3.87	1.82

Table 3-5. Thermal Diffusivity Results from the Mixture Models Overall and by Sediment Layer

Method	α_3 (cm^2/s)	α_9 (cm^2/s)	α_{20} (cm^2/s)	$\alpha_{overall}$ (cm^2/s)
Volume Average	0.0067	0.0059	0.0060	0.0068
Zang	0.0058	0.0048	0.0048	0.0056
Campbell	0.0125	0.0138	0.0137	0.0146

mixture models to an overall thermal diffusivity makes it possible to compare the results with the results from SEDMOD.

Table 3-6 shows the parameter estimation results of each isolation technique using SEDMOD. Only one thermal diffusivity value is shown per simulation because SEDMOD assumes the bed is a homogenous slab of material. The table shows the isolation method used, the season in which the temperature data were collected, the estimated thermal diffusivity (α), and the upper and lower confidence bounds based on the critical sum of squares calculations. Notice while the confidence bounds of the summer fabric simulation come very close to the laboratory measurement, the only simulation whose confidence limits bound the laboratory value is the aluminum cap.

Table 3-6. Results from SEDMOD Conduction Model. Thermal Diffusivity Is Shown With the Calculated Confidence Bounds

			Confidence Bounds	
Isolation Method	**Season**	**α (cm^2/s)**	**Bottom (cm^2/s)**	**Top (cm^2/s)**
No Cylinder SEDMOD	Summer	0.0246	0.0226	0.0267
No Cylinder SEDMOD	Fall	0.0217	0.0153	0.0323
Open Cylinder SEDMOD	Summer	0.041	0.0379	0.0444
Fabric Cylinder SEDMOD	Summer	0.0074	0.0069	0.0088
Fabric Cylinder SEDMOD	Fall	0.0103	0.0084	0.0128
Aluminum Cylinder SEDMOD	Fall	0.0064	0.0054	0.0076

Even though the confidence bounds of the fabric capped simulation do not include the measured thermal diffusivity the calculated confidence limits cannot be trusted implicitly. The residuals plots show that the data does not exactly fit the basic assumption that the variance is constant (Appendix D). Bearing this in mind the fabric capping method could be as viable as the aluminum capping method as its estimate and bounds are close to the laboratory measurement.

SEDMOD results were also plotted against the observed temperature time-series to view the ability of the model to approximate temperatures throughout the sediment (Figure 3-6). The SEDMOD results seem to best fit the observed temperatures using the data from the aluminum capped cylinder (Figure 3-6(a)) followed by the fabric capped data (Figure 3-6(b)) and the no cylinder data (Figure 3-6(c)).

Discussion

The main objective of this research is to compare the results of both mixture models and SEDMOD in order to recommend the method that best approximates streambed conduction parameters. This judgment will be made based on a direct comparison to measured laboratory values.

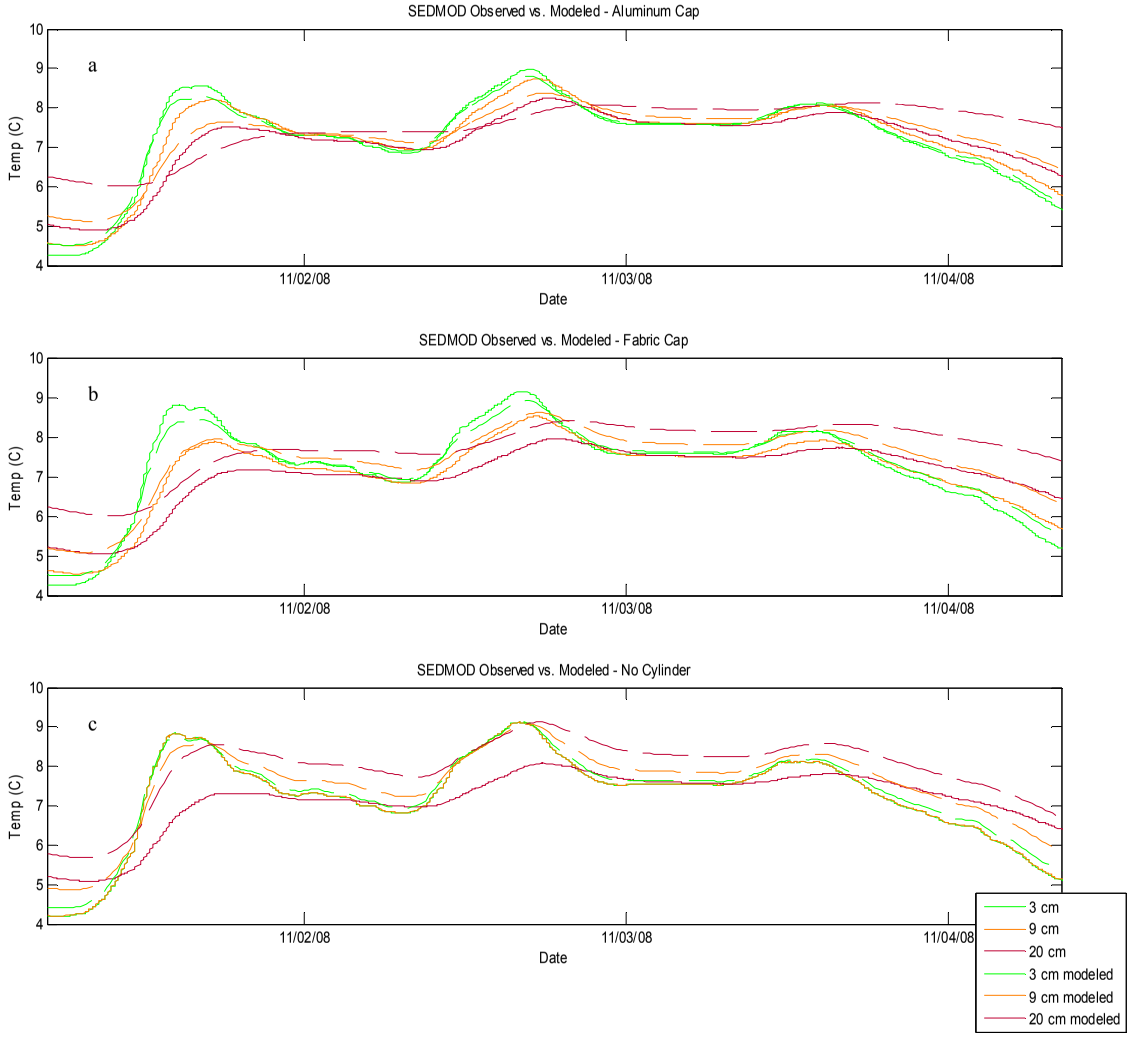

Figure 3-6. Plotted comparison of observed temperature data (solid) with SEDMOD output (dashed). Aluminum cap (a), Fabric Cap (b), No Cylinder (c).

Though the laboratory value is a measured property, it should be understood that there is error in these results. One source of error may be due to the fact that the measurements were not taken in situ. Sediments were dug up, processed, and remixed in a different orientation which could transfer heat differently. Also, the heated probe technique used provides a value for its point of insertion and not the slab of material. The temperature at which the thermal conductivity was measured (19°C) is also a source of error as the sediment temperatures during the experiment generally were cooler (3-15°C). In order to treat this concern, a literature search was performed to approximate the effects that a 15 ºC temperature difference would have on thermal diffusivity. Ozisik [1993] shows the thermal diffusivity range for limestone (the principal mineral in Curtis Creek) from 100 – 300 ºC as 0.0056 – 0.0059 cm^2/s. Since a change of 200ºC only produced a change of 0.0003 cm^2/s and the model results are reported to 0.0001 cm^2/s, it was assumed that the effects of a 15 ºC difference between the laboratory measurements and the field would be negligible.

There are also many other dynamic processes that may be in the stream but were absent during the laboratory measurements (e.g., interaction of a larger sediment volume, stream water chemistry, etc.). The application of only three heat capacity measurements to all of the sediment samples is also a source of error as the bed material is not uniform in size or composition.

The first modeling group to be compared to the laboratory results is that of mixture models. In considering Table 3-4, the volume weighted average gives the best approximation of thermal conductivity at all three sample depths, followed closely by Zang, and then Campbell at almost double the laboratory conductivity measurement.

After calculating an overall thermal diffusivity using these three models, the volume weighted average approximation matches the laboratory value. Zang's method is the next best approximation, varying from the laboratory value about 20%, and Campbell's method differs from the laboratory by almost a factor of three. While the volume weighted average method matches the lab value exactly this method is somewhat suspect. Volume averaging properties such as density and specific heat is fairly common as their properties generally change as a function of volume. On the other hand, when considering thermal conduction, heat will follow the path of least resistance, or in other words will "short circuit" through materials of higher conductivity around those of lower thermal conductivity. Therefore, using the volume weighted average of thermal conductivity requires further research to verify the robustness of this method of calculating overall conductivity/diffusivity of a material.

Campbell's method of estimating total thermal conductivity may be appealing because it requires no assumption of the thermal conductivity of the materials and requires only bulk density and volumetric water content which can be measured easily. This method, however, far overestimated the thermal conductivity (and therefore diffusivity) of the bed sediments.

The data from both Figure 3-4 and Figure 3-5 were used to calibrate SEDMOD. Table 3-6 shows that the only simulation whose confidence bounds include the laboratory thermal diffusivity is the data from the aluminum capped cylinder. It is interesting to note that the results show that the degree to which the method limited exchange was the degree to which an accurate approximation was reached. For example the aluminum capping method excluded vertical and horizontal exchange and thus approximated the

thermal diffusivity closest to the laboratory measurement (α = 0.0064 cm^2/s). The fabric capping method stopped exchange in the horizontal direction, and limited it in the vertical direction, which also gave a reasonable approximation *(*α = 0.0074 cm^2/s). This trend changes with the open cylinder and no cylinder techniques. The open cylinder limits horizontal exchange and the no cylinder limits none, nevertheless, the open cylinder produces the least accurate thermal conductivity (α = 0.041 cm^2/s and 0.0217 cm^2/s, respectively). Figure 3-6 corroborates these numerical approximations. The simulation that gives the thermal diffusivity that best matches the laboratory also matches the observed temperatures more closely.

Even though the aluminum capping method returns statistically accurate results the amount of error in the calibration data and model results should be considered. The HOBO® Temp Pro V2 temperature probes have a stated accuracy of 0.2 ºC, and even though much effort went into minimizing the error induced by the installation techniques, these methods did somewhat change the orientation of the bed. The errors from instrumentation or installation techniques could be a reason that SEDMOD did not exactly mimic the calibration data. Further error is shown by the 3 cm aluminum capped temperatures following the main channel temperature while the fabric cap exhibits a decreased amplitude and time lag (Figure 3-4). This could be due to the 3 cm probes from the fabric and aluminum capped cylinders being switched or solar radiation heating the aluminum cap and increasing the temperature of the shallow sediments.

There were further concerns with the methods that allowed vertical exchange across the temperature sensors (e.g., fabric capped cylinder and open cylinder). SEDMOD results from the summer fabric cap simulation are closer to the laboratory than

those of the fall. This could be due to hydrologic changes such as increased downwelling in the fall. This is supported by the fact that the no cylinder method also exhibited an increase in estimated thermal diffusivity in the fall. A second hypothesis is based on field observations of the fabric when installed. Initially the geo-fabric only allowed water to "weep" through it, but when installed the second time in the fall, water flowed freely through the fabric. The change may be due to weathering of the fabric after months of installation in the stream. In order to view if the summer installation of the fabric was isolating conductive heating, the SEDMOD simulation results were plotted against the observed sediment temperatures (Figure 3-7).

The comparison of these data show that the observed temperatures have a lower amplitude and a longer time lag than the 3 cm conduction predictions of SEDMOD. The 9 cm predictions of SEDMOD are much better, but at 20 cm SEDMOD produces lower amplitude temperatures. This suggests that the fabric was allowing some advective flows through the cylinder which increased heat transfer through the cylinder. Not accounting for this advective heat transfer, SEDMOD resulted in a slightly higher thermal diffusivity estimate in an effort to match the data. This method merits further study to test different sections of the time-series to see if it yields accurate estimates. Additionally, data collected in different locations using this method could also test how water depth or seepage rates affect the ability to estimate thermal diffusivity using this method.

The sensitivity of SEDMOD to the initial and boundary conditions is shown by difference in the model results before and after the changes to SEDMOD. Prior to changing to an initial temperature input, SEDMOD was run using the data from the

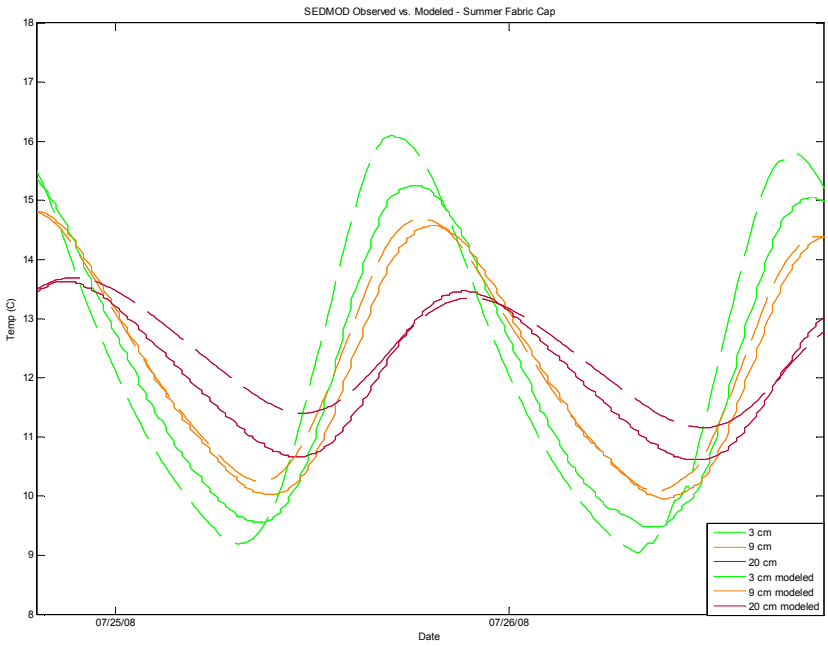

Figure 3-7. Comparison of SEDMOD summer fabric simulation results. Green line represents 3 cm depth, orange 9 cm, and brown 20 cm. Dotted line represents model results while the solid line represents the observed temperature data.

aluminum capped cylinder. The model results were 0.0212 cm^2/s, almost three times the measured laboratory value. This shows that SEDMOD is very sensitive to the bottom boundary temperature assigned. After the change, SEDMOD statistically matches the laboratory value when a reasonable ground temperature is used. It is recommended that future applications monitor ground temperature at a specific depth and incorporate it into the model to get the most representative results.

Table 3-7 shows an overview of all of the thermal diffusivity approximations for each modeling method considered in this paper. All methods except SEDMOD show values for each sediment layer, and SEDMOD shows one overall estimate for the bed sediments.

The methods that best approximate the thermal diffusivity of each layer are the volume weighted average and Zang's method. Comparing the overall results for the streambed, the two methods that best approximate the thermal diffusivity are the volume weighted mixture model and SEDMOD using the aluminum and fabric capping technique. The volume weighted average matches the laboratory value in this study and when the confidence bounds are considered, SEDMOD (aluminum and fall fabric) also provides a reasonable approximation of the laboratory value.

Conclusions

In comparing the mixture model results, the volume weighted average method yields the best approximation of both thermal conductivity and diffusivity. As such, the volume weighted average method is recommended as the most accurate mixture model to estimate thermal conductivity and diffusivity using sediment sample and literature data.

There is question to the ability of using volume weighted averaging to predict thermal conductivity, as this property does not depend on the volume of the sample. Further research is recommended to verify the ability of this technique to return consistently accurate results.

Table 3-7. Results Summary. This Table Shows All of the Thermal Diffusivity Results from Each of the Models and Lab for Comparison

Method		Temperature (ºC)	α_3 (cm^2/s)	α_9 (cm^2/s)	α_{20} (cm^2/s)	Overall α (cm^2/s)
Mixing Model	Volume Average	N/A	0.0067	0.0059	0.006	0.0068
	Zang		0.0058	0.0048	0.0048	0.0056
	Campbell		0.0125	0.0138	0.0137	0.0146
SEDMOD	No Cylinder	4				0.0217
	Open Cylinder	12				0.041
	Fabric	12				0.0074
	Aluminum	6				0.0064
Laboratory		19	0.0075	0.0059	0.007	0.0068

The data collection method that yielded the best approximation of thermal diffusivity was the aluminum capped cylinder. SEDMOD used with the temperature data from the fabric capped cylinder should also be considered as a possible method. The change in accuracy over time exhibited with the fabric capping method should be reiterated. Further research is needed to study the accuracy of this technique when new fabric is installed for short periods of time. It is also recommended that future data collection efforts incorporate a measure of ground temperatures in order to set a representative bottom boundary for the model.

A last consideration in selecting from these methods is the expense in both time and money required for each method. Sediment sampling is very time intensive and soil sieves are required. Samples must be collected, sieved, dried, weighed, and volumes measured. Data required for conduction modeling also has some expense depending on the temperature sensors used, but requires less of a time commitment to get the data ready for modeling. In short, one needs to consider the resources available to them and judge accordingly when making a data collection and model decisions.

CHAPTER 4

CONCLUSIONS

Streambed conduction parameters are required for various efforts to model hydrologic processes in streams. Different approaches are used to calculate or estimate thermal properties for these studies. Even with the wide spread use of these approaches, little has been done to compare and contrast the different modeling methods and their associated data collection methods. As part of this research, data collection methods were created in order to estimate streambed conduction properties. Streambed sediment samples were collected and literature values for sediment thermal properties were found to calculate thermal conductivity of the bed using mixture models. Methods of isolating temperature variation due to conduction only were tested using steel cylinders with different capping materials to eliminate advective flow. These temperature data were used as calibration data for the bed conduction model SEDMOD. The results of the different model applications were compared to laboratory measurements to determine their accuracy.

Data were collected on Curtis Creek to identify the most representative sediment temperature sampling methods that represent heating due to conduction. Of the installation techniques for the sediment temperature probe arrays, Installation Method 2 (spike installation technique) yielded the results that induced the least amount of preferential flow. It was adopted in the subsequent data collection stages and is recommended as the best practice for monitoring in situ sediment temperature variation due to both hyporheic exchange and bed conduction.

To isolate temperature variability due to conduction, temperature probe arrays installed using this method were surrounded by a steel cylinder with two different capping materials. While the fabric capping technique yielded results less influenced by advection than the cylinder technique used previously by *Neilson et al.* [2009], it still permitted some advective flow through the cylinder which may affect its use in conduction modeling. The aluminum capping technique is the only technique explored in this research that did indeed limit all advective flow from the channel; however, the results may have been influenced by heating due to solar radiation. Further research is recommended to test the theory of heating by solar radiation. The data collected from the sediment sampling and vertical hydraulic gradients yielded information that proved to aid in understanding the temperature results.

In comparing the mixture model results, the volume weighted average method yields the best approximation of both thermal conductivity and diffusivity. As such, the volume weighted average method is recommended as the most accurate mixture model to estimate thermal conductivity and diffusivity using sediment samples and literature data. There is question to the ability of using volume weighted averaging to predict thermal conductivity, as this property does not depend on the volume of the sample. Further research is recommended to verify the ability of this technique to return consistently accurate results.

The process based modeling portion of this research compares the different data collection methods used to calibrate SEDMOD. The data collection method that yielded the best approximation of thermal diffusivity using SEDMOD was the aluminum capped cylinder. SEDMOD used with the temperature data from the fabric capped cylinder

should also be considered as a possible method. The change in accuracy over time exhibited with the fabric capping method should be reiterated. Further research is needed to study the accuracy of this technique when new fabric is installed for short periods of time. It is also recommended that future data collection efforts incorporate a measure of ground temperatures in order to set a representative bottom boundary for the model.

A last consideration in selecting from these methods is the expense in both time and money required for each method. Sediment sampling is very time intensive and soil sieves are required. Samples must be collected, sieved, dried, weighed, and volumes measured. Conduction modeling methods also have some expense depending on the temperature sensors used, but requires less of a time commitment to get the data ready for modeling. In short, one needs to consider the resources available to them and judge accordingly when making a data collection and model decisions.

CHAPTER 5

ENGINEERING SIGNIFICANCE

This research brings much to the field of Environmental Engineering by the way of adding innovative data collection techniques and model adaptations to the engineering toolkit. The first benefit of this work is the description of data collection methods and the comparison of techniques for estimating thermal properties of sediments. This will help in the selection of the most representative models, and guide experimental design.

By following the recommendations of using either the volume weighted mixture modeling method or the SEDMOD conduction model in conjunction with the aluminum capped isolation technique, more accurate estimates of streambed thermal conduction parameters can be established. A better estimate of these parameters can provide for a better approximation of other stream processes. By fixing the conduction properties, advective exchange rates can be estimated more accurately [*Constantz et al.*, 2002; *Constantz*, 2008; *Hatch et al.*, 2006]. In the past these fluxes have been neglected or vaguely defined [*Constantz and Thomas*, 1996; *Silliman and Booth*, 1993; *Stonestrom and Blasch*, 2003], but if quantified can assist in instream temperature predictions.

More accurate instream temperature predictions will allow for more appropriate management decisions to be made. A possible benefit can be found on Curtis Creek itself. Curtis Creek is home to the Bonneville Cutthroat Trout which has been named as a "species of interest" by the State of Utah [*Harja*, 2006]. Trout are sensitive to water temperature changes and by using these sediment modeling techniques in conjunction with a temperature model, managers could more accurately predict future temperatures

and make better informed management decisions favorable to the Bonneville Cutthroat. For example, in the past the Utah Division of Wildlife Resources (DWR) has allowed some controlled grazing of Curtis Creek. The DWR also diverts a portion of Curtis Creek to provide irrigation water as well as stock water at the ranch. Estimated bed conduction parameters from the methods described in this research could be used with an instream temperature model to predict the water temperature effects of increased solar radiation due to the removal of tall grasses through grazing in the riparian zone. The temperature model could be used further to approximate how much of the stream could be diverted without having detrimental temperature affects on the Bonneville Cutthroat population. Actions such as these could use the methods described herein to improve water resource management in Utah and throughout the world.

CHAPTER 6

RECOMMENDATIONS FOR FUTURE RESEARCH

This work has uncovered several possible topics for future research, including:

1. Repeat collection of isolated temperature time-series at different locations:
    a. Collect data at shaded locations as well as those exposed to solar radiation to study the effects of solar radiation on the aluminum capping technique.
    b. Study the ability of the geo-fabric cap to produce accurate diffusivity estimates under different conditions (e.g., vertical head gradient, water depth, etc.).
2. While collecting isolated data from Recommendation 1, collect ground temperatures at 1 m depth below the stream in order to integrate these into the conduction model.
    a. Alter the code of SEDMOD to incorporate the new 1m depth time-series and test the ability to accurately estimate thermal diffusivities by incorporating these data.
    b. Collect ground temperatures (at 1 m depth) at several locations along the stream to discover whether this superficial groundwater temperature varies at different points along the stream.

3. Collect streambed sediment samples from different streams and apply the volume weighted average model to test its ability to consistently estimate thermal conductivity.

REFERENCES

Allen, J. D. (1995), *Stream Ecology: Structure and Function of Running Waters*, 400 pp. Chapman & Hall, New York.

Andrews, F., and G. Rodvey (1980), Heat exchange between water and tidal flats, *D.G.M*, *24*(2).

ASTM (2005), ASTM E 1269 Standard Test Method for Determining Specific Heat Capacity by Differential Scanning Calorimetry, 6 pp.

ASTM (2007), D-422 - 63 Standard Test Method for Particle-Size Analysis of Soils, 8 pp.

ASTM (2008), D5334 - 08 Standard Test Method for Determination of Thermal Conductivity of Soil and Soft Rock by Thermal Needle Probe Procedure, 8 pp.

Baxter, C., and F. R. Hauer (2003), Measuring Groundwater-Stream Water Exchange: New Techniques for Installing Minipiezometers and Estimating Hydraulic Conductivity, *Trans. Am. Fish. Soc.*, *132*, 493-502.

Bejan, A. (1993), *Heat Transfer*, Wiley, New York.

Berthouex, P. M., and L. C. Brown (2002), *Statistics for Environmental Engineers*, 489 pp., Lewis Publishers, New York.

Boyd, M., and B. Kasper (2003), Analytical methods for dynamic open channel heat and mass transfer: Methodology for heat source model Version 7.0.

Brigaud, F., and G. Vasseur (1989), Mineralogy, porosity and fluid control on thermal conductivity of sedimentary rocks, *Geophys. J.*, *98*, 528-542.

Campbell, G. S. (1985), *Soil physics with BASIC: transport models for soil-plant systems*, 3 ed., Elsevier.

Carslaw, H. S., and J. C. Jaeger (1959), *Conduction of Heat in Solids*, 510 pp., Oxford Press, Oxford, UK.

Cengel, Y. A. (1998), *Heat Transfer: A Practical Approach*, McGraw-Hill, New York.

Cengel, Y. A., and M. A. Boles (2002), *Thermodynamics: An Engineering Approach*, 930 pp., McGraw-Hill Higher Education, Boston.

Chapra, S., G. Pelletier, and H. Tao (2004), "QUAL2K: A modeling framework for simulating river and stream water quality (Version 1.3): Documentation and Users Manual." Civil and Environmental Engineering Dept., Tufts University, Medford.

Chapra, S. (2006), Sediment-Water Heat Exchange in Surface Water Quality Models, B. T. Neilson, ed.

Chow, V. T., D.R. Maidment, and L.W. Mays (1988), *Applied Hydrology*, 572 pp. McGraw-Hill, New York.

Constantz, J., and C. L. Thomas (1996), The use of streambed temperature profiles to estimate the depth, duration, and rate of percolation beneath arroyos, *Water Resour. Res.*, *32*(12), 3597-3602.

Constantz, J. (1998), Field study and simulation of diurnal temperature effects on infiltration and variably saturated flow beneath an ephemeral stream, *Water Resour. Res.*, *34*(9), 2137-2153.

Constantz, J., A.E. Stewart, R. Niswonger, and L. Sarma (2002), Analysis of temperature profiles for investigating stream losses beneath ephemeral channels, *Water Resour. Res.*, *38*(12).

Constantz, J. (2008), Heat as a tracer to determine streambed water exchanges, *Water Resour. Res.*, *44*.

DeVries, D. A. (1963), Thermal properties of soils, in *Physics of the Plant Environment*, edited by W. R. V. Wijk, pp. 211-235, Elsevier, New York.

Evans, E. C., G.R. McGregor, and G.E. Petts (1998), River energy budgets with special reference to river bed processes, *Hydrol. Processes*, *12*(4), 575-595.

Geiger, R. (1965), *The Climate Near the Ground*, 611 pp., Harvard University Press, Cambridge.

Grigull, U., and H. Sandner (1984), *Heat Conduction*, p. 75-86, Springer-Verlag, New York.

Harja, J. (2006), Hyrum City Blacksmith Fork hydroelectric project, Office of the Govenor, Salt Lake City, Utah.

Hatch, C. E., A.T. Fisher, J. Revenaugh, J. Constantz, and C. Ruehl (2006), Quantifying Surface water-groundwater interactions using time series analysis of streambed thermal records: Method development, *Water Resour. Res.*, *42*, 1-14.

Healy, R. W., and A. D. Ronan (2003), Documentation of Computer Program VS2DH for Simulation of Energy Transport in Variably Saturated Porous Media--Modification of the U.S. Geological Survey's Computer Program VS2DT, edited by USGS. < http://pubs.er.usgs.gov/usgspubs/wri/wri964230>.

Hondzo, M., C.R. Ellis, and H.G. Stefan (1991), Vertical diffusion in small stratified lake: Data and error analysis, *J. Hydraulic Eng.*, *117*(10), 1352-1369.

Hondzo, M., and H. G. Stefan (1994), Riverbed heat conduction prediction, *Water Resour. Res.*, *30*(5), 1503-1513.

Horai, K.-i. (1971), Thermal Conductivity of Rock-Forming Minerals, *J. Geophys. Res.*, *76*(5), 1278-1308.

Hutchinson, G. E. (1957), *A Treatise on Limnology*, 1015 pp., Wiley, New York.

Incropera, F. P., D.P. Dewitt, T.L. Bergman, and A.S. Lavine (2007), *Fundamentals of Heat and Mass Transfer*, 6 ed., 995 pp., Wiley, New York.

Jobson, H. E. (1977), Bed conduction Computation for Thermal Models, *J. Hydraulics Div., ASCE, 103(10)*, 1213-1217.

Lee, J.-Y., and J.-S. Hahn (2006), Characterization of groundwater temperature obtained from the Korean national groundwater monitoring stations: Implications for heat pumps., *J. Hydrology*, *329*, 514-526.

Mills, A. F. (1992), *Heat Transfer*, 916 pp, Irwin, Homewood, IL.

Morse, W. L. (1970), Stream Temperature Prediction Model, *Water Resour. Res.*, *6*, 290-301.

Nakshabandi, G. A., and H. Kohnke (1965), Thermal conductivity and diffusivity of soils as related to moisture tension and other physical properties, *Agr. Met.*, *2*, 271-279.

Neilson, B. (2006), Dynamic stream temperature modeling: Understanding the causes and effects of temperature impairments and uncertainty in predictions, edited, p. 178, Utah State University, Merrill-Cazier Library, Special Collections.

Neilson, B. T., D.K. Stevens, S.C. Chapra, and C. Bandaragoda (2009), Data Collection Methodology for Dynamic Temperature Model Testing and Corroboration, *Hydrol. Processes*.

Or, D., M. Tuller, and J.M Wraith (2008), *Agricultural & Environmental Soil Physics*, 226 pp., USU Copy Center, Logan.

Ozisik, M. N. (1993), Physical properties, in *Heat Conduction*, p. 659, Wiley, New York.

Poole, G. C., and C. H. Berman (2001), An ecological perspective on in-stream temperature: Natural heat dynamics and mechanisms of human-caused thermal degradation, *Environ. Manage.*, *27*(6), 787-802.

Ronan, A. D., D.E. Prudic, C.E. Thodal, and J. Constantz (1998), Field study and simulation of diurnal temperature effects on infiltration and variably saturated flow beneath an ephemeral stream, *Water Resour. Res.*, *34*(9), 2137-2153.

Silliman, S. E., and D. F. Booth (1993), Analysis of time-series measurements of sediment temperature for identification of gaining vs. losing portions of Juday Creek, Indiana, *J. Hydrology*, *146*, 131-148.

Sinokrot, B. A., and H. G. Stefan (1993), Stream Temperature Dynamics: Measurements and Modeling, *Water Resour. Res.*, *29*(7), 2299-2312.

Sinokrot, B. A., and H. G. Stefan (1994), Stream Water-Temperature Sensitivity to Weather and Bed Parameters, *J. Hydraulic Eng.*, *120*, 722-736.

Stonestrom, D. A., and K. W. Blasch (2003), Determining temperature and thermal properties for heat-base studies of surface-water ground-water interaction, *U.S Geol. Survey Circular*, *1260*, 73-80.

Tindall, J. A., J.R. Kunkel, and D.E. Anderson (1999), Transport of heat and gas in soil and at the surface, in *Unsaturated Zone Hydrology for Scientists and Engineers*, edited, p. 624, Prentice-Hall, Englewood Cliffs, NJ.

Touloukian, Y. S., and E. H. Buyco (1970), Thermophysical properties of matter, in *Thermal Conductivity of Nonmetallic Solids*, edited by Y. S. Touloukian and C. Y. Ho, p. 1649, Plenum, New York.

Tsay, T.-K., G.J. Ruggaber, S.W. Effler, C.T. Driscoll (1992), Thermal Stratification Modeling of Lakes with Sediment Heat Flux, *J. Hydraulic Eng.*, *118*(3), 407-419.

USGS (2003), Heat as a tool for studying the movement of ground water near streams, United States Geological Survey, Reston, VA.

Webb, B. W., and Y. Zang (1997), Spatial and Seasonal Variability in the Components of the River Heat Budget, *Hydrol. Processes*, *11*, 79-101.

Zang, H. F., X.S. Ge, H. Ye, and D.S. Jiao (2007), Heat conduction and heat storage characteristics of soils, *Applied Thermal Eng.*, *27*, 369-373.

Zhuo, X. (2009), Temporal and spatial thermal flux analysis for estimating vertical fluxes of a high-gradient rock-mountain streambed, 8 pp, Unpublished Manuscript.

APPENDICES

APPENDIX A

Sediment Measurements X96 - 240

X96 Sediment Data			
Depth (cm)	**Size (cm)**	**Weight (g)**	**V_f^* (mL)**
0 - 7.5	6.350	4634	1700
	2.540	4054.7	1521
	1.270	1700.7	640
	0.635	1121	460
	0.475	343.2	130
	0.238	750.6	370
	0.084	1177.7	560
	0.021	1340.3	510
	0.005	80.5	23
7.5 - 15	6.350	2414	915
	2.540	2792.6	1065
	1.270	2312.7	835
	0.635	1877.7	700
	0.475	637.9	260
	0.238	1254.5	505
	0.084	1776.6	880
	0.021	1777.2	682
	0.005	181.5	52.5
15 - 22.5	6.350	4667.7	1869
	2.540	719	266
	1.270	1347.2	503
	0.635	1173.1	453
	0.475	410.2	177
	0.238	855.1	368
	0.084	1147.1	569
	0.021	926.1	374
	0.005	76.8	42.5

* V_f = Volume of the sample material of the given size.

X240 Sediment Data			
Depth (cm)	**Size (cm)**	**Weight (g)**	**V_f^* (mL)**
0 - 7.5	6.350	3053.3	220
	2.540	2114.5	800
	1.270	1920.6	746
	0.635	1895.5	710
	0.475	651.4	230
	0.238	1146.8	416
	0.084	771	319
	0.021	442.6	250
	0.005	92.5	42
7.5 - 15	6.350	6013.8	2312
	2.540	1209.6	432
	1.270	851.9	322
	0.635	463.5	335
	0.475	1024.5	179
	0.238	1078.9	408
	0.084	1114.4	445
	0.021	557.5	250
	0.005	79.2	16
15 - 22.5	6.350	1363.7	509
	2.540	2156.4	777
	1.270	1552.8	565
	0.635	2248.7	822
	0.475	916.3	332
	0.238	2026.2	719
	0.084	1924.7	825
	0.021	925.6	436
	0.005	99.5	37

* V_f = Volume of the sample material of the given size.

X713 Sediment Data			
Depth (cm)	**Size (cm)**	**Weight (g)**	**V_f^* (mL)**
0 - 7.5	6.350	3135.3	1150
	2.540	4020.6	1466
	1.270	1740.2	630
	0.635	1349.8	488
	0.475	525.7	195
	0.238	1148.7	402
	0.084	427.8	148
	0.021	240.2	100
	0.005	69.5	23
7.5 - 15	6.350	4561.1	1498
	2.540	2241.9	802
	1.270	1969.6	653
	0.635	1644	593
	0.475	546.4	200
	0.238	1338.9	403
	0.084	1461.3	598
	0.021	627.2	412
	0.005	154.4	60
15 - 22.5	6.350	1462	509
	2.540	2125.9	770
	1.270	2328	840
	0.635	2485.8	908
	0.475	793.1	297
	0.238	2189.6	811
	0.084	2186.8	909
	0.021	824.9	310
	0.005	181.5	72

* V_f = Volume of the sample material of the given size.

X995 Sediment Data			
Depth (cm)	**Size (cm)**	**Weight (g)**	**V_f^* (mL)**
0 - 7.5	6.350	4063.1	1477
	2.540	2127.7	805
	1.270	2054.5	773
	0.635	1577.8	604
	0.475	421	178
	0.238	743.5	269
	0.084	571.5	228
	0.021	462.1	196
	0.005	89.2	53
7.5 - 15	6.350	561.6	213
	2.540	2083.1	739
	1.270	2120	751
	0.635	2128.4	768
	0.475	763.1	263
	0.238	1535.3	568
	0.084	1406.1	544
	0.021	707.6	285
	0.005	155.8	67
15 - 22.5	6.350	425	151
	2.540	2480.9	888
	1.270	1810.1	663
	0.635	1849.4	660
	0.475	718.1	245
	0.238	1480.1	559
	0.084	682.5	272
	0.021	1743.1	673
	0.005	228.2	100

* V_f = Volume of the sample material of the given size.

X1160 Sediment Data			
Depth (cm)	**Size (cm)**	**Weight (g)**	**V_f^* (mL)**
0 - 7.5	6.350	N/A	N/A
	2.540	5688.1	2097
	1.270	2886	1068
	0.635	1932.4	734
	0.475	622.8	215
	0.238	1247.1	467
	0.084	1245.4	530
	0.021	605.1	266
	0.005	158.1	66
7.5 - 15	6.350	N/A	N/A
	2.540	3452.1	1295
	1.270	1467.9	1000
	0.635	1326.4	815
	0.475	358.7	340
	0.238	750.2	714
	0.084	1035.9	1036
	0.021	1971.2	735
	0.005	207.1	58
15 - 22.5	6.350	N/A	N/A
	2.540	1154.6	430
	1.270	1467.9	555
	0.635	1326.4	526
	0.475	358.7	175
	0.238	750.2	300
	0.084	1035.9	559
	0.021	1197.2	490
	0.005	207.1	69

* V_f = Volume of the sample material of the given size.

APPENDIX B

Sediment Measurements and Calculations for X995

X995 Sediment Data

Depth (cm)	Size (cm)	Weight (g)	V_f^* (mL)	k (W/(m*°C))	Cp (J/(g*°C))	ρ_b^{**} (g/m^3)	Vf/Vs# (Unitless)	$\rho_t^{\wedge}$ (g/m^3)	Φ (Unitless)
0 - 7.5	6.350	4063.1	1477	2.15	0.909	2.751	0.266	2.354	0.176
	2.540	2127.7	805	2.15	0.909	2.643	0.145		
	1.270	2054.5	773	2.15	0.909	2.658	0.139		
	0.635	1577.8	604	2.15	0.909	2.612	0.109		
	0.475	421	178	2.15	0.909	2.365	0.032		
	0.238	743.5	269	2.15	0.909	2.764	0.048		
	0.084	571.5	228	2.5	0.8	2.507	0.041		
	0.021	462.1	196	2.5	0.8	2.358	0.035		
	0.005	89.2	53	2.5	0.8	1.683	0.010		
	Water	976.7069	977	0.058	4.1921	0.9997	0.176		
7.5 - 15	6.350	561.6	213	2.15	0.909	2.637	0.038	2.306	0.245
	2.540	2083.1	739	2.15	0.909	2.819	0.133		
	1.270	2120	751	2.15	0.909	2.823	0.135		
	0.635	2128.4	768	2.15	0.909	2.771	0.138		
	0.475	763.1	263	2.15	0.909	2.902	0.047		
	0.238	1535.3	568	2.15	0.909	2.703	0.102		
	0.084	1406.1	544	2.5	0.8	2.585	0.098		
	0.021	707.6	285	2.5	0.8	2.483	0.051		
	0.005	155.8	67	2.5	0.8	2.325	0.012		
	Water	1361.591	1362	0.058	4.1921	0.9997	0.245		
15 - 22.5	6.350	425	151	2.15	0.909	2.815	0.027	2.296	0.243
	2.540	2480.9	888	2.15	0.909	2.794	0.160		
	1.270	1810.1	663	2.15	0.909	2.730	0.119		
	0.635	1849.4	660	2.15	0.909	2.802	0.119		
	0.475	718.1	245	2.15	0.909	2.931	0.044		
	0.238	1480.1	559	2.15	0.909	2.648	0.101		
	0.084	682.5	272	2.5	0.8	2.509	0.049		
	0.021	1743.1	673	2.5	0.8	2.590	0.121		
	0.005	228.2	100	2.5	0.8	2.282	0.018		
	Water	1348.595	1349	0.058	4.1921	0.9997	0.243		

* V_f = Volume of the sample material of the given size.

^ ρ_t = Overall Density (Including water and sediment) $\rho_t = \sum \left[\rho_b \cdot \frac{V_f}{V_s} \right] + \rho_{water} \cdot \frac{V_{water}}{V_s}$

Vf/Vs = Ratio of fraction volume over the sample section (e.g., 5560 mL per sample section).

** ρ_b is dry bulk density of the sediment mixture.

APPENDIX C

Critical Sum of Squares Calculations for SEDMOD Simulations

Aluminum Cap - Critical Sum of Squares

$$246.97 = 244.3307 + 244.3307 \cdot \left(\frac{1}{356-1} \cdot 3.84 \right)$$

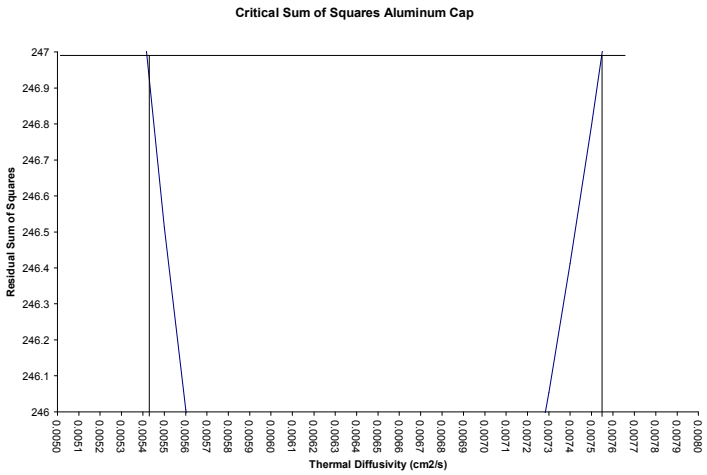

Bounds: 0.0054 – 0.0076

Fall Fabric Cap - Critical Sum of Squares

$$253.77 = 251.057 + 251.057 \cdot \left(\frac{1}{357-1} \cdot 3.84 \right)$$

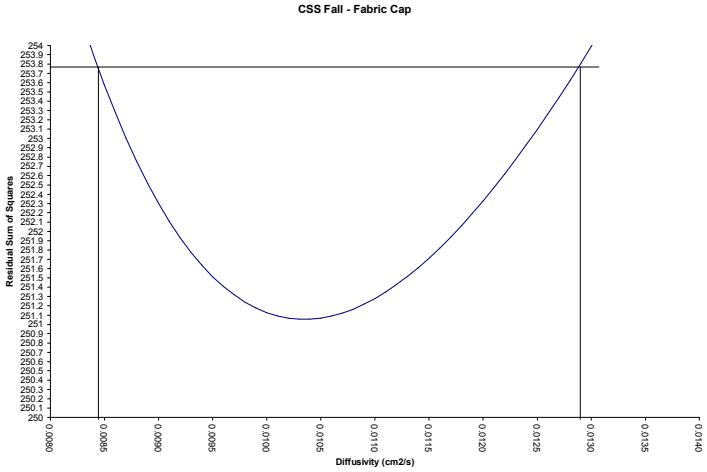

Bounds: 0.0084 – 0.0128

Summer Fabric Cap - Critical Sum of Squares

$$309.42 = 306.38 + 306.38 \cdot \left(\frac{1}{388 - 1} \cdot 3.84 \right)$$

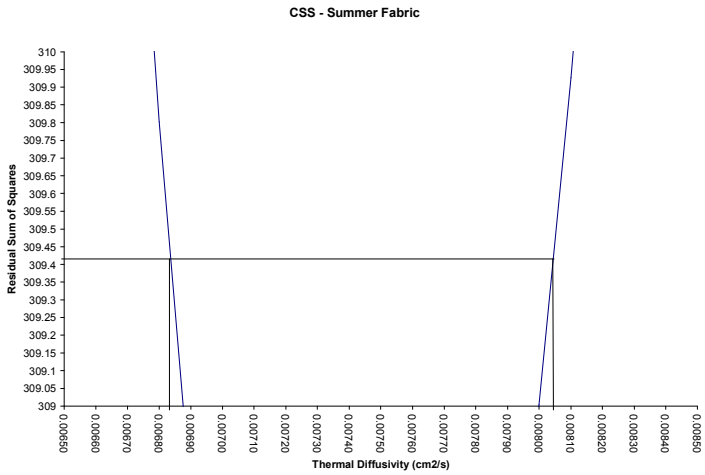

Bounds: 0.00685 – 0.00885

Fall No Cap No Cylinder - Critical Sum of Squares

$$348.135 = 344.42 + 344.42 \cdot \left(\frac{1}{358 - 1} \cdot 3.84 \right)$$

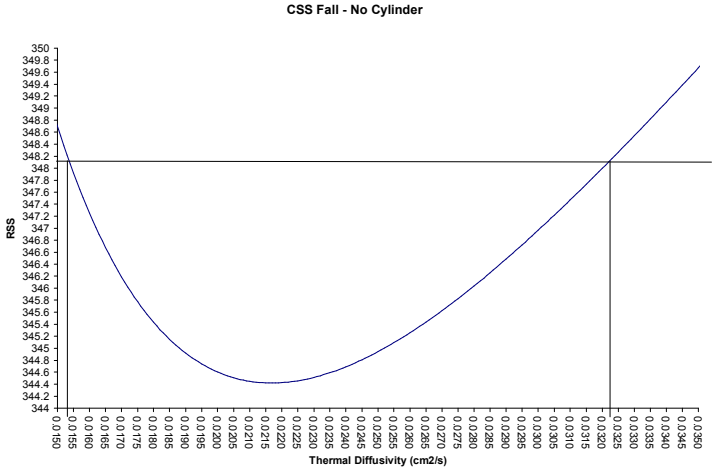

Bounds: 0.0153 – 0.0323

Summer No Cap No Cylinder - Critical Sum of Squares

$$183.36 = 181.42 + 181.42 \cdot \left(\frac{1}{359 - 1} \cdot 3.84 \right)$$

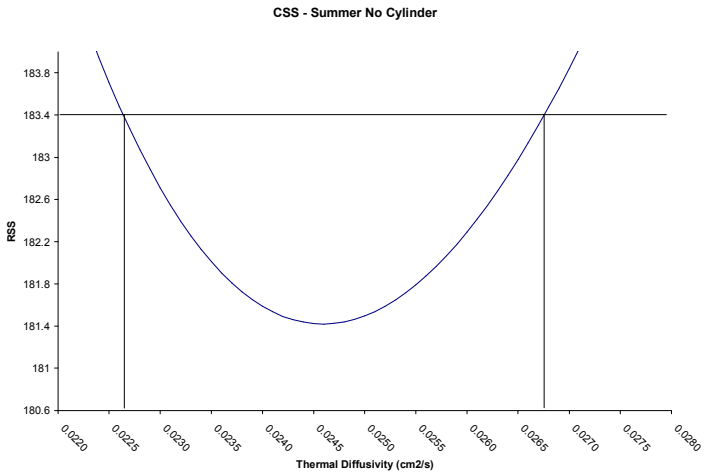

Bounds: 0.0226 – 0.0267

Open Cylinder - Critical Sum of Squares

$$193.89 = 191.9848 + 191.9848 \cdot \left(\frac{1}{388 - 1} \cdot 3.84 \right)$$

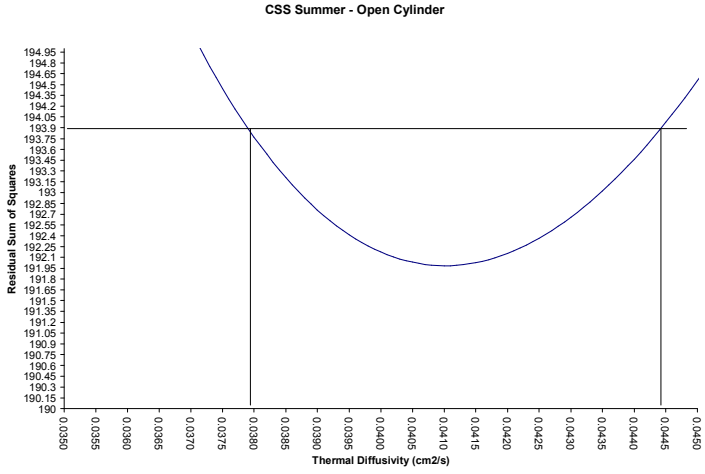

Bounds: 0.0378 – 0.0444

APPENDIX D

Residual Plots of SEDMOD Simulations

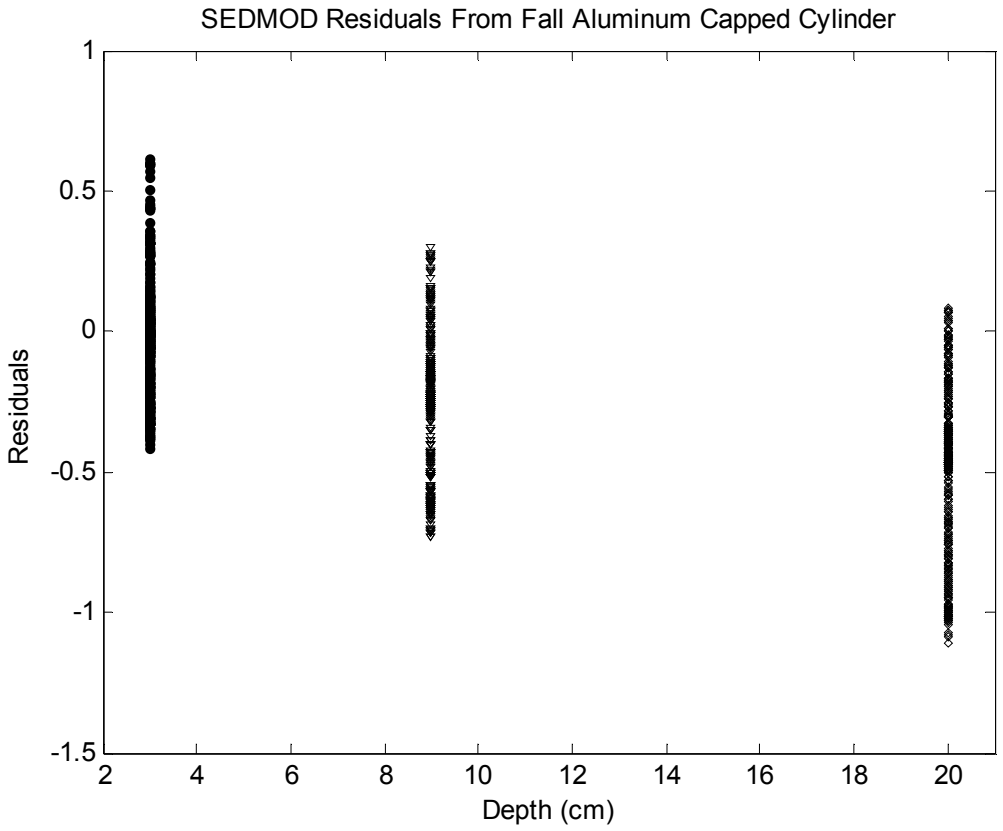
SEDMOD Residuals From Fall Aluminum Capped Cylinder
Residuals
Depth (cm)
1
0.5
0
-0.5
-1
-1.5
2
4
6
8
10
12
14
16
18
20

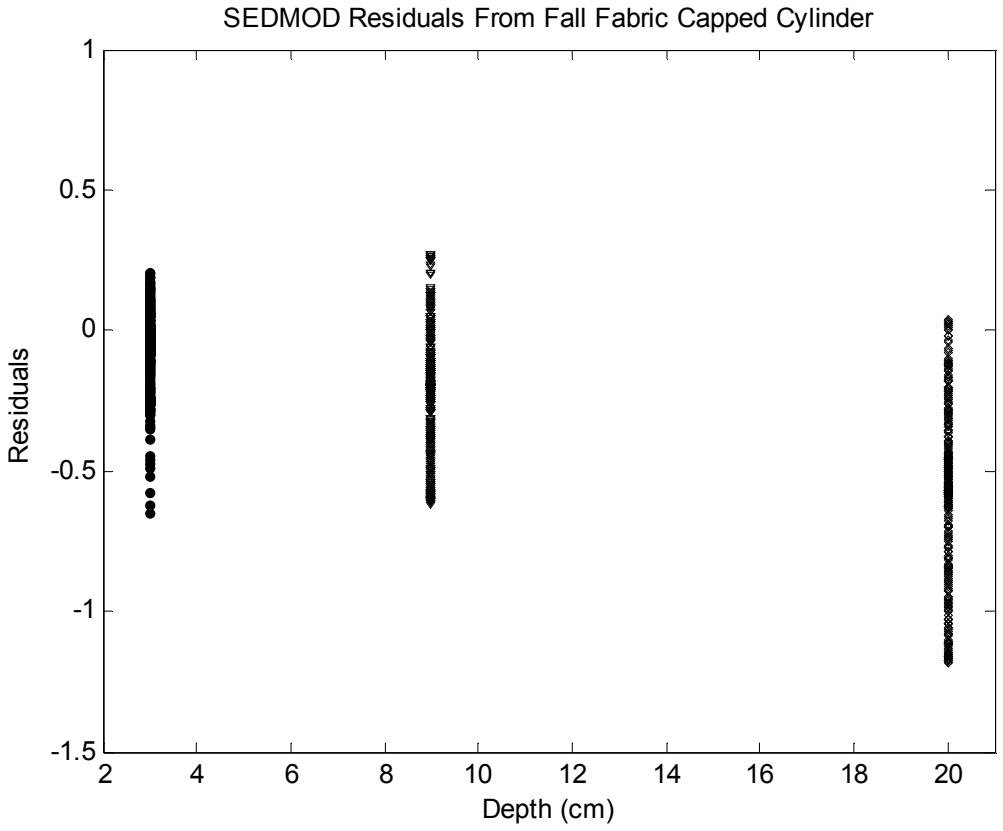
SEDMOD Residuals From Fall Fabric Capped Cylinder
Residuals
Depth (cm)
1
0.5
0
-0.5
-1
-1.5
2
4
6
8
10
12
14
16
18
20

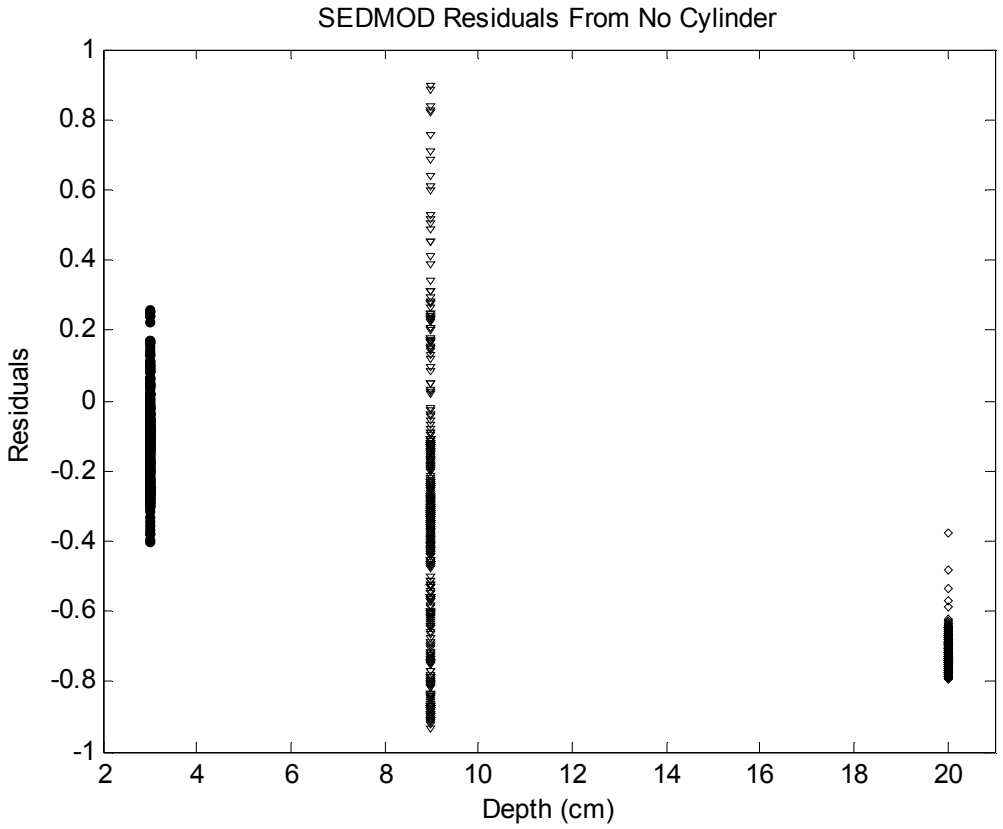
SEDMOD Residuals From No Cylinder
Residuals
Depth (cm)
1
0.8
0.6
0.4
0.2
0
-0.2
-0.4
-0.6
-0.8
-1
2
4
6
8
10
12
14
16
18
20

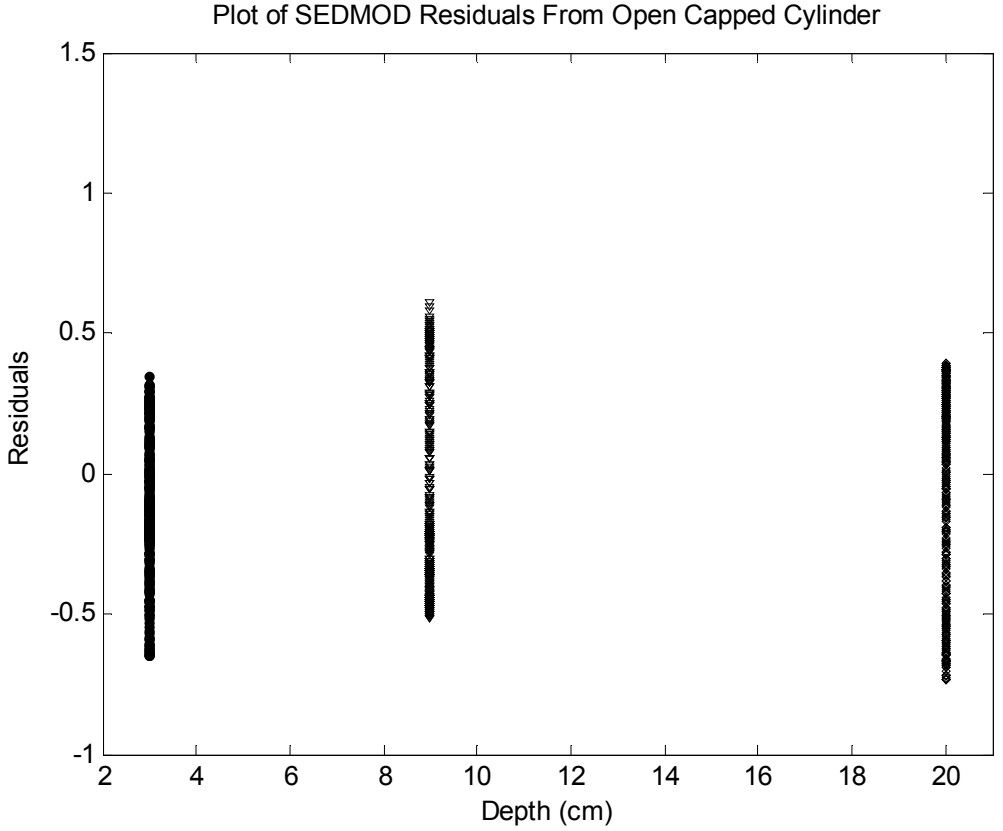
Plot of SEDMOD Residuals From Open Capped Cylinder
Residuals
Depth (cm)
1.5
1
0.5
0
-0.5
-1
2
4
6
8
10
12
14
16
18
20